NASA CONTRACTOR REPORT

NASA CR-2409

NASA CR-2409

EVALUATION OF A METAL SHEAR WEB SELECTIVELY REINFORCED WITH FILAMENTARY COMPOSITES FOR SPACE SHUTTLE APPLICATION

by J. H. Laakso and J. W. Straayer

Prepared by
BOEING AEROSPACE COMPANY
Seattle, Wash. 98124
for Langley Research Center

NATIONAL AERONAUTICS AND SPACE ADMINISTRATION • WASHINGTON, D. C. • AUGUST 1974

1. Report No.	2. Government Accession No.	3. Recipient's Catalog No.
NASA CR- 2409		

4. Title and Subtitle	5. Report Date
Evaluation of a Metal Shear Web Selectively Reinforced With Filamentary Composites For Space Shuttle Application— Final Report	August 1974
	6. Performing Organization Code Orgn. 2-5560

7. Author(s)	8. Performing Organization Report No.
J. H. Laakso and J. W. Straayer	D180-17969-1
9. Performing Organization Name and Address Boeing Aerospace Company Research and Engineering Division P.O. Box 3999 Seattle, Washington 98124	10. Work Unit No. 11. Contract or Grant No. NAS1-10860
12. Sponsoring Agency Name and Address National Aeronautics and Space Administration Washington, D.C. 20546	13. Type of Report and Period Covered Contractor Report 14. Sponsoring Agency Code

15. Supplementary Notes

Final Report

This program was sponsored by the Design Technology Branch.

16. Abstract

A final program summary is given for test and evaluation activities that were conducted under Phase III of NASA/Langley Research Contract NAS 1-10860, *Evaluation of a Metal Shear Web Selectivity Reinforced with Filamentary Composites for Space Shuttle Application.* Three large scale advanced composite shear web components were tested and analyzed to evaluate application of advanced composite shear web construction to a Space Shuttle Orbiter thrust structure. The shear web design concept consisted of a titanium-clad $\pm 45^{\circ}$ boron/epoxy web laminate stiffened with vertical boron/epoxy reinforced aluminum stiffeners and longitudinal aluminum stiffening. The design concept was evaluated to be efficient and practical for the application that was studied. Because of the effects of buckling deflections, a requirement is identified for shear buckling resistant design to maximize the efficiency of highly-loaded advanced composite shear webs.

17. Key Words (Suggested by Author(s))	18. Distribution Statement
Shear Web Composite Selective Reinforcement Metal-Clad Composite Space Shuttle	Unclassified - Unlimited STAR Category: 32

19. Security Classif. (of this report)	20. Security Classif. (of this page)	21. No. of Pages	22. Price*
Unclassified	Unclassified	78	$4.00

*For sale by the National Technical Information Service, Springfield, Virginia 22151

Page Intentionally Left Blank

FOREWORD

This report is a final technical program report prepared by the Research and Engineering Division, Boeing Aerospace Company, under NASA Contract NAS 1-10860, *Evaluation of a Metal Shear Web Selectively Reinforced with Filamentary Composites For Space Shuttle Application.* The program was sponsored by the Design Technology Branch of the Langley Research Center. The report covers contract activities during the period of May 1971 to October 1973.

Performance of the contract was under the management of Mssrs. D. K. Zimmerman and J. W. Straayer, Structures Development and Analytical Methods Group; Mr. John H. Laakso was the Technical Leader.

The authors wish to acknowledge the contributions of the following program participants:

D. D. Smith	Design
Dr. R. E. Sherrer	Analysis
M. M. House	Structural Testing
P. W. Poggel	Test Instrumentation
D. Lee	Test Data Processing
B. C. Dykes	Moire Fringe Instrumentation
J. T. Hoggatt	Materials and Processes
D. R. Gieseking	Manufacturing
R. Nelson	Manufacturing
M. Ice	Computing

Special acknowledgement is made to the Langley Research Center for program guidance and to the Grumman Aerospace Corporation for furnishing structural design and loads information on their Space Shuttle orbiter configurations.

Page Intentionally Left Blank

TABLE OF CONTENTS

Page Intentionally Left Blank

LIST OF FIGURES

LIST OF SYMBOLS

B/E	Boron/epoxy composite material
P	Applied Beam Load
ϵ_B	Out-of-plane plate bending strain
N_{MF}	Moire fringe order index
$D_{11}, D_{12}, D_{22}, D_{33}$	Orthotropic plate bending stiffnesses
EI_T	Transverse stiffener bending stiffness
EI_L	Longitudinal stiffener bending stiffness
GJ_T	Transverse stiffener torsional stiffness
$Z_{B/E}$	Coordinate of extreme B/E ply from laminate mid-plane surface
W	Out-of-plane web plate deflection
V	Total web shear load
N_x	Distributed web plate load in x-direction
N_y	Distributed web plate load in y-direction
N_{xy}	Distributed web plate shear load
P_c	Beam chord load
ϵ_c	Beam chord strain
ϵ_p	Web plate strain at nominal panel height
$\mu\epsilon$	Units for microstrain
H	Full web structural depth
H_e	Effective web depth for general instability analysis
H_{PANEL}	Nominal web laminate height
S_S	Transverse stiffener spacing
L_x	Panel buckle mode width parameter
L_y	Panel buckle mode length parameter
θ	Panel buckle mode skin angle parameter
Units	Customary units are stated first and SI units follow in parentheses.

EVALUATION OF A METAL SHEAR WEB SELECTIVELY REINFORCED WITH FILAMENTARY COMPOSITES FOR SPACE SHUTTLE APPLICATION—FINAL REPORT

By J. H. Laakso and J. W. Straayer
Boeing Aerospace Company

1.0 INTRODUCTION

This report presents the component testing and evaluation results of a program for the development of a practical advanced composite shear web concept which is a candidate for near-term application to primary flight vehicle structure. The program consisted of three phases:

Phase I	Shear Web Design Development
Phase II	Shear Web Component Fabrication
Phase III	Shear Web Component Structure Testing and Analysis

In Phase I [1], the Space Shuttle orbiter main engine thrust beam structure was selected for the shear web application study area because of (1) the high shear loading occurring in this area and (2) the potential importance of weight savings to the Space Shuttle System. The high shear loading and beam bending strains in this area, with the structure at essentially room temperature, makes the use of B/E reinforcement advantageous. In addition, the thrust structure has large total weight and is located in an area where weight savings assist in vehicle balancing. The center-loaded thrust beam was selected for study from an early orbiter configuration and has basic dimensions of 40 in. deep by 200 in. span (1 m x 5.1 m). Design development was then performed which involved computer-aided design and analysis, detailed design evaluation, testing of unique and critical details, and structural test planning. Particular emphasis was placed on computer-aided design to screen candidate concepts. Various web design concepts having both boron/epoxy reinforced and all-metal construction were synthesized by a computer-aided adaptive random search procedure programmed as the Boeing OPTRAN code.

A practical shear web was identified by the design concept evaluation study in Phase I. This concept has a titanium-clad ±45° boron/epoxy web plate with vertical boron/epoxy reinforced aluminum stiffeners.

Preliminary detailed thrust beam drawings using the B/E reinforced design concept and an all-titanium construction were prepared in Phase I; weight trades and cost analysis were conducted using these drawings. These studies showed a 24% savings with the selected concept relative to an all-metal construction. Cost per pound of mass savings was estimated to be less than $250 (551 $ US/kg). Critical details and reliability considerations for the B/E reinforced design were identified and structural element tests were made to substantiate the design details. Cyclic load and temperature design environments were simulated in some of the element tests. A significant outcome of the element test program was the determination of titanium cladding reinforcement required to preclude failure at joints and fastener holes. Two small scale shear web elements 18 in. by 25 in. (45.7 cm x 63.5 cm) were also tested to demonstrate the performance of the basic web laminate details.

Phase II [2] activities were oriented primarily toward the fabrication of three large scale B/E reinforced shear web test components. The test webs were 36 in. high by 47 in. long (0.9 m x 1.2 m). Test fixtures for the shear web test elements and the large scale web components were also fabricated during Phase II. The center-loaded beam test fixture was configured so that the test web components could be installed in one half of the beam for each test. The test fixtures were fabricated from available standard extruded aluminum sections and plates.

Phase III [3] was concerned with structural analysis and testing of the three B/E reinforced shear web components. The first web design was established from the baseline B/E reinforced shear web design developed in Phase I. Slight changes were made in web depth and stiffener details to simplify fabrication of the test web. Based on the static test results of the first test web, improvements in analysis and fabrication procedures were made to enhance shear buckling resistance.

The second test web was tested to demonstrate fatigue resistance; 400 loadings to a simulated limit load level were applied with no apparent fatigue damage resulting in spite of high prebuckling deformations. After post-test analysis, the second test web was delivered to the Langley Research Center.

The third test web, shown in Figure 1 was redesigned using an improved computer-aided design procedure. Provision for longitudinal stiffening and buckling analyses based on discrete stiffening were added to the OPTRAN code used in Phase I; weight trades conducted with the code indicated that longitudinal stiffening would be beneficial. The

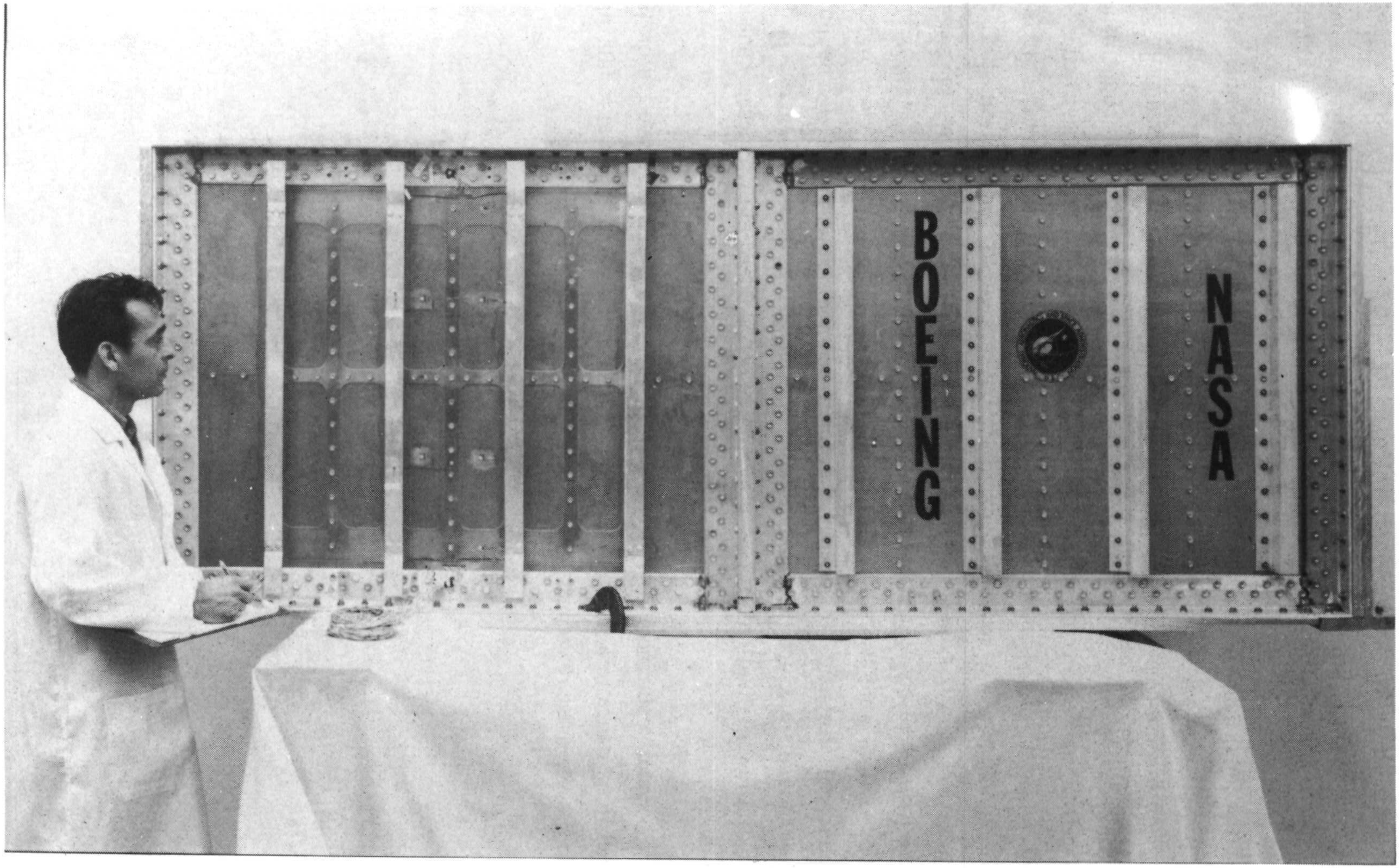

Figure 1: THIRD SHEAR WEB COMPONENT TEST ASSEMBLY

static strength test results for the third web indicated that performance of the design concept was significantly improved by the additional stiffening and was strongly dependent on shear buckling resistance qualities.

Because of the importance of prebuckling deformations to load carrying performance, an approximate prebuckling analysis procedure was studied and incorporated in the OPTRAN code for the B/E reinforced web concept. Weight trades were then conducted using the OPTRAN code to establish correlation with the third test web and final weight comparisons between the B/E reinforced concept and all-metal construction. The final weight trades for production hardware load conditions indicated the B/E reinforced web concept offers a theoretical nominal section weight saving of 31% compared to conventional stiffened titanium construction; with edge joint and other design detail weight penalties considered, the B/E reinforced web concept offers weight savings on the order of 24%. Several design configuration options were also studied including the use of all-aluminum stiffeners, instead of B/E reinforced stiffeners, to stiffen a B/E reinforced web plate; use of all-aluminum stiffeners was found to reduce theoretical nominal weight savings from 31% to 28% in the cases studied (a lower-bound on stiffener effectiveness was assumed in these design concept variation studies).

This report presents a summary of test and evaluation results which were selected on the basis of their importance to a future production program. All program data and results may be found in the respective references for the three program phases [1,2,3].

2.0 SUMMARY

Large scale structural testing was conducted on three 36 in. high by 47 in. long (0.9 m x 1.2 m) shear web components having titanium-clad ±45° B/E web plates stiffened with vertical B/E reinforced aluminum stiffeners and, in the case of the third web, a longitudinal aluminum stiffener. The results of the shear web tests are summarized below:

TEST WEB	MAXIMUM LOAD LB (MN)	RESULTS
1	540,000 (2.4)	Failed by composite panel fracture in postbuckling condition.
2	530,000 (2.36)	No failure at maximum load after loaded 400 times to 400,000 lb (1.78 MN). Web had large prebuckle strains during fatigue loading Web was in postbuckled condition in final loading
3	575,000 (2.56)	Failed by composite panel fracture in a panel that was in a prebuckled condition

The third web had significantly more stiffening than the first and second webs and displayed what can be called "shear resistant" response which allowed higher loading. The integrity of the fatigue test web, test web 2, was unaffected by the degree of prebuckling strains that occurred during the cyclic limit loading. Based on analyses of the test data and other computed optimum design cases, the ultimate allowable composite strain in prebuckled panels will generally govern the strength of highly loaded stiffened composite shear web configurations of the type studied in this program.

Based on the results of the large scale component testing and analysis, the shear web concept is evaluated to be practical and efficient for the application that was studied. However, because of the importance of prebuckling deformations and related hazards of low post-buckling strength, the composite reinforced design concept will require more sophisticated structural analysis than in the case of conventional metal web for a production hardware application.

3.0 SHEAR WEB TEST COMPONENTS

3.1 FABRICATED COMPONENT DESIGN DETAILS

The design concept and details of the test web components are illustrated in Figures 2, 3 and 4. These illustrations show in general how local web laminate reinforcement and composite load transfer were provided for.

An objective in selecting the actual test web configurations was to have large size and realistic design details so that evaluation of the design concept could be made without scaling problems. Consequently, the test web laminates were sized 36 in. high by 47 in. long (0.9 m x 1.2 m). The web laminate cladding reinforcement scheme is highlighted by the completed laminate section shown in Figure 5 and dimensioned in Figure 6; except for the transverse stiffener spacing and the presence of the longitudinal stiffener, the general details of the test web laminates were similar. The cladding skins, as shown in Figure 6, had three thicknesses formed by chem-milling: (1) a "nominal panel cladding thickness" of about 0.020 in. (0.51 mm) forming a nominal panel height of 25 in. (64 cm), (2) a "reinforced cladding thickness" of about 0.050 in. (1.3 mm) which extends from the nominal panel edge to the beam chord members giving a clear web height of 29 in. (74 cm), and (3) a "full stock sheet cladding thickness" of 0.063 in. (1.6 mm) in the web edge and end bay areas. It is the reinforced cladding thickness that provided local reinforcement to the web laminate along stiffener lines and in step-lap joint areas as shown in Figures 3 and 4. A close-up view of the typical laminate edge joint details is shown in Figure 7.

The typical stiffener subassembly parts are shown in Figures 8 and 9.

The test web components were assembled in one-half of a center-loaded test beam fixture for testing; the three test beam assemblies are shown in Figures 10 (test web 1), 11 (test web 2), 1 (test web 3) and 14 (test web 3). Longitudinal stiffener details associated with test web 3 are presented in Figures 12 and 13.

The materials used in the test web components are listed in Figure 15. Aluminum (7075-T6) was used in the test beam framework and conventional high strength steel fasteners were employed for assembly of all test beam parts.

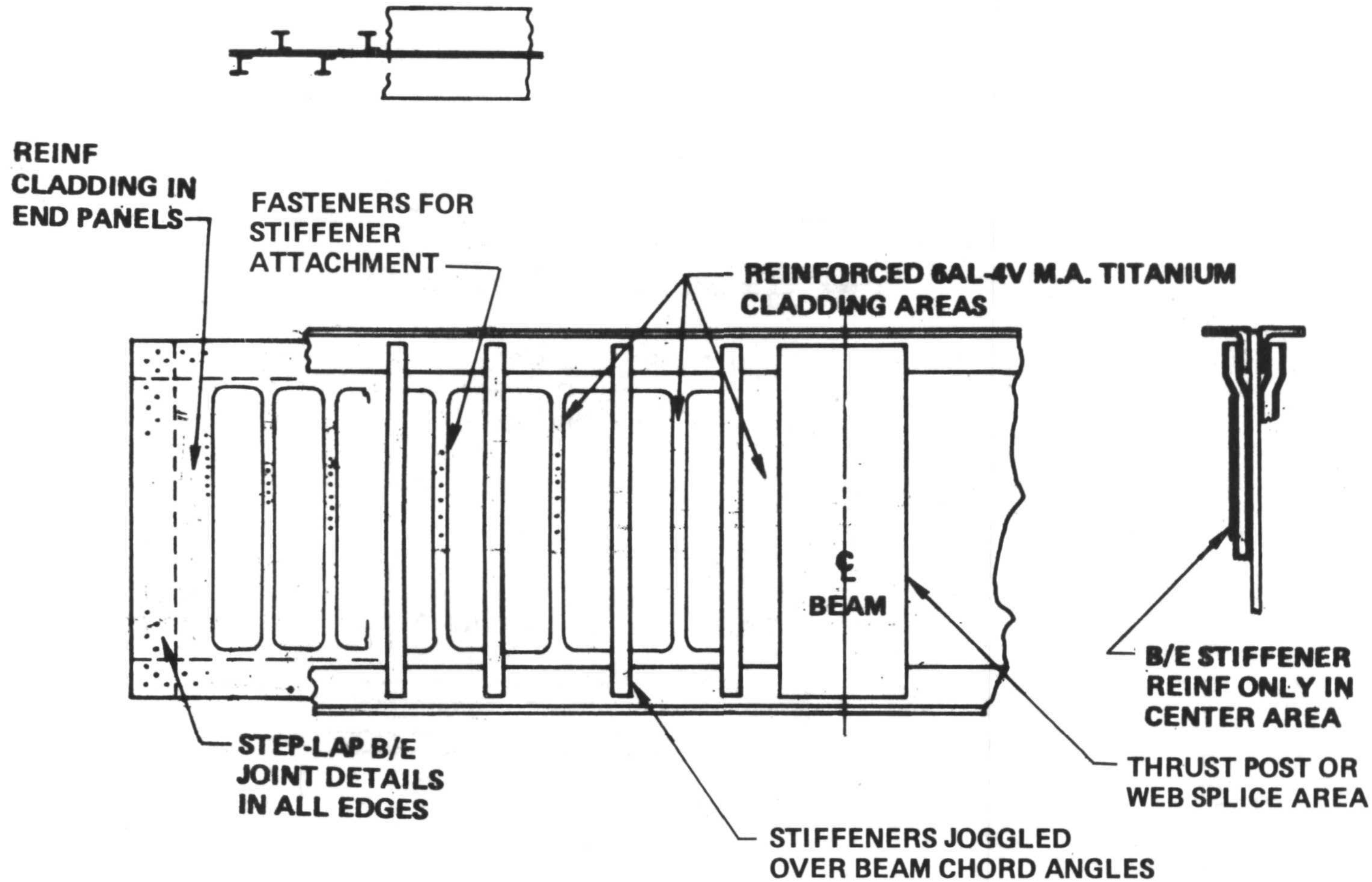

Figure 2: B/E REINFORCED SHEAR WEB DESIGN CONCEPT

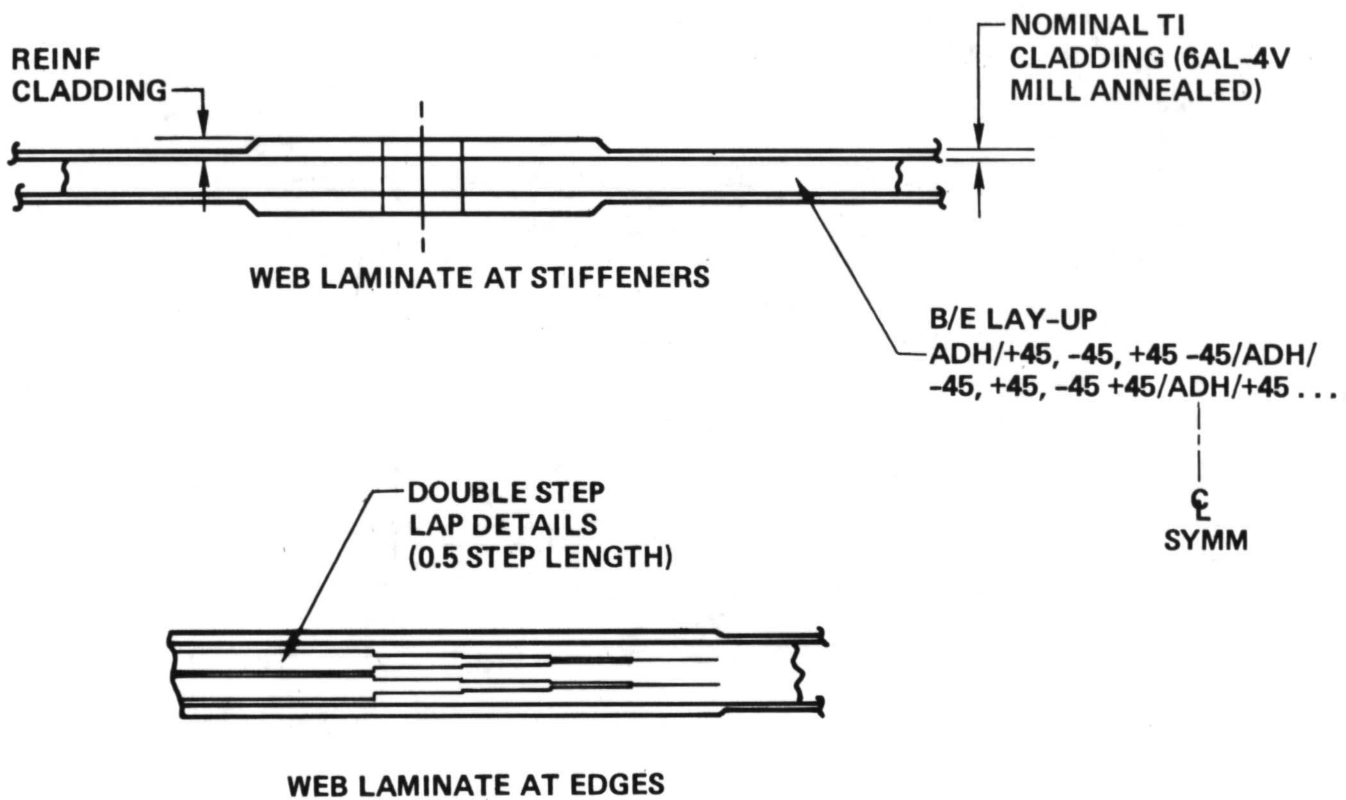

Figure 3: B/E REINFORCED SHEAR WEB DESIGN DETAILS

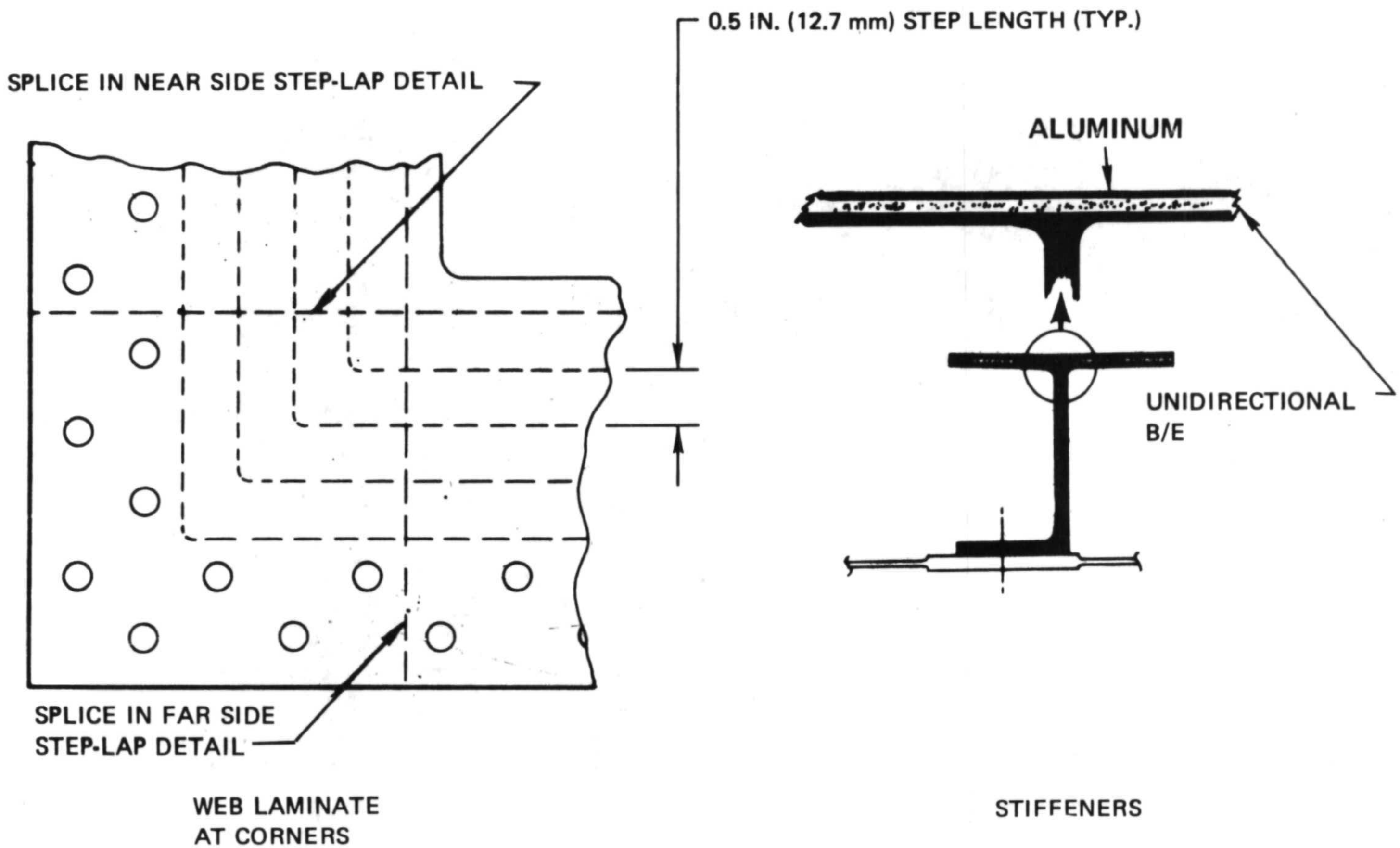

Figure 4: B/E REINFORCED SHEAR WEB DESIGN DETAILS

Figure 5: TEST WEB 3 LAMINATE SECTION

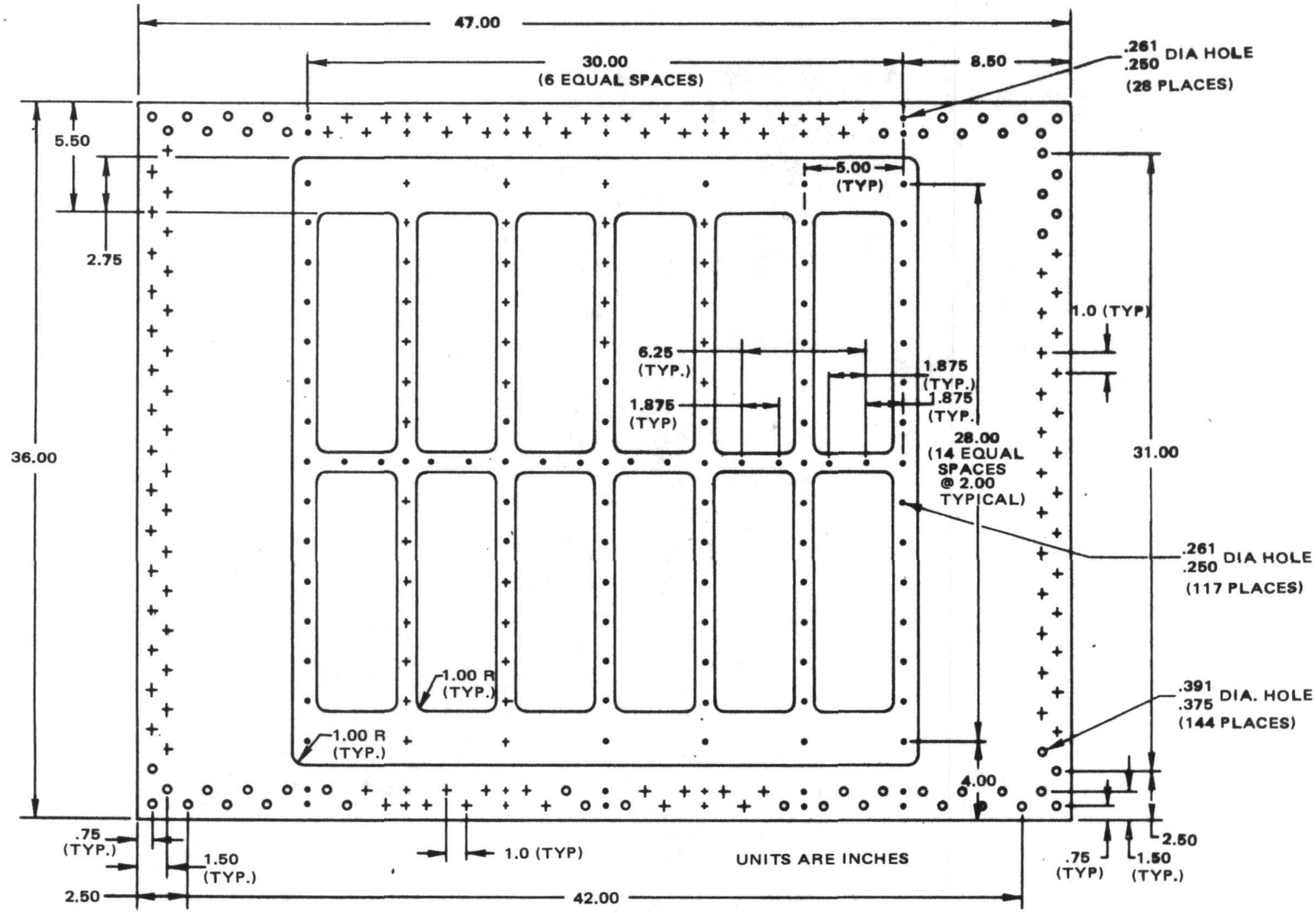

Figure 6: TEST WEB 3 LAMINATE CLADDING DETAILS

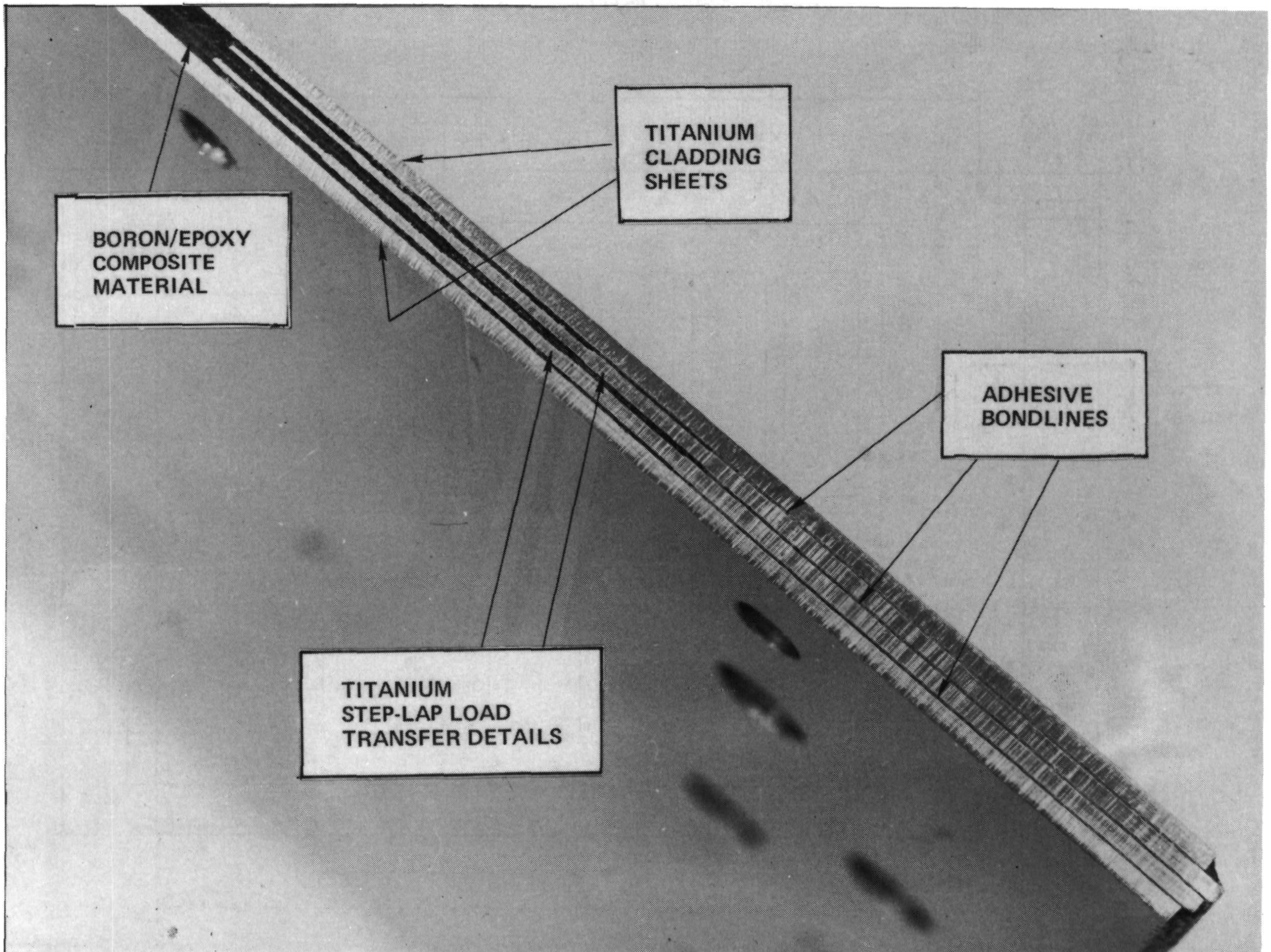

Figure 7: WEB LAMINATE EDGE JOINT SECTION

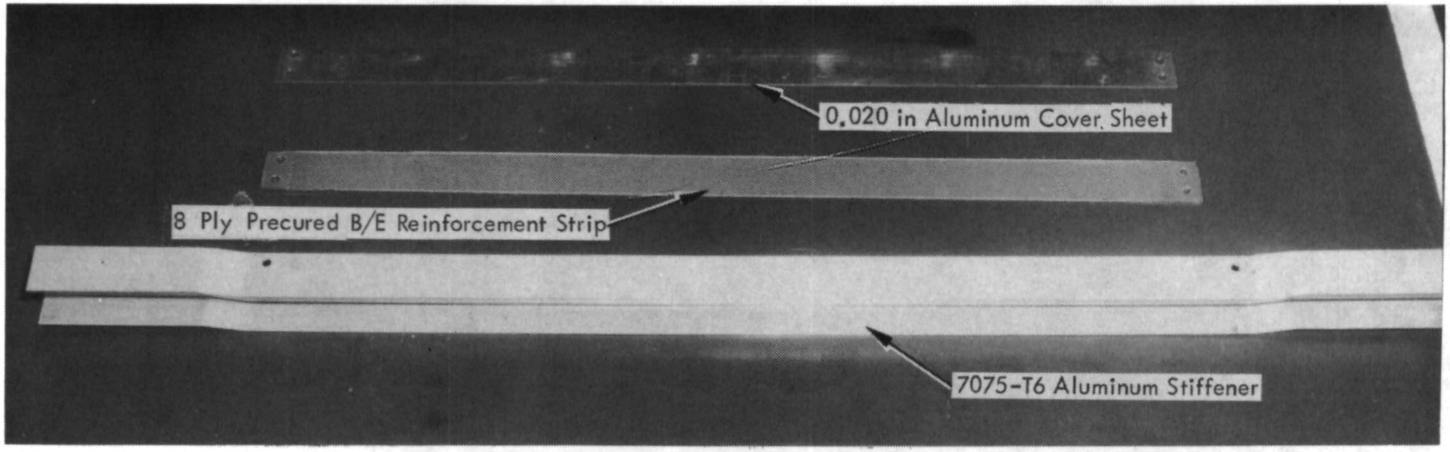

Figure 8: ***TRANSVERSE STIFFENER PARTS***

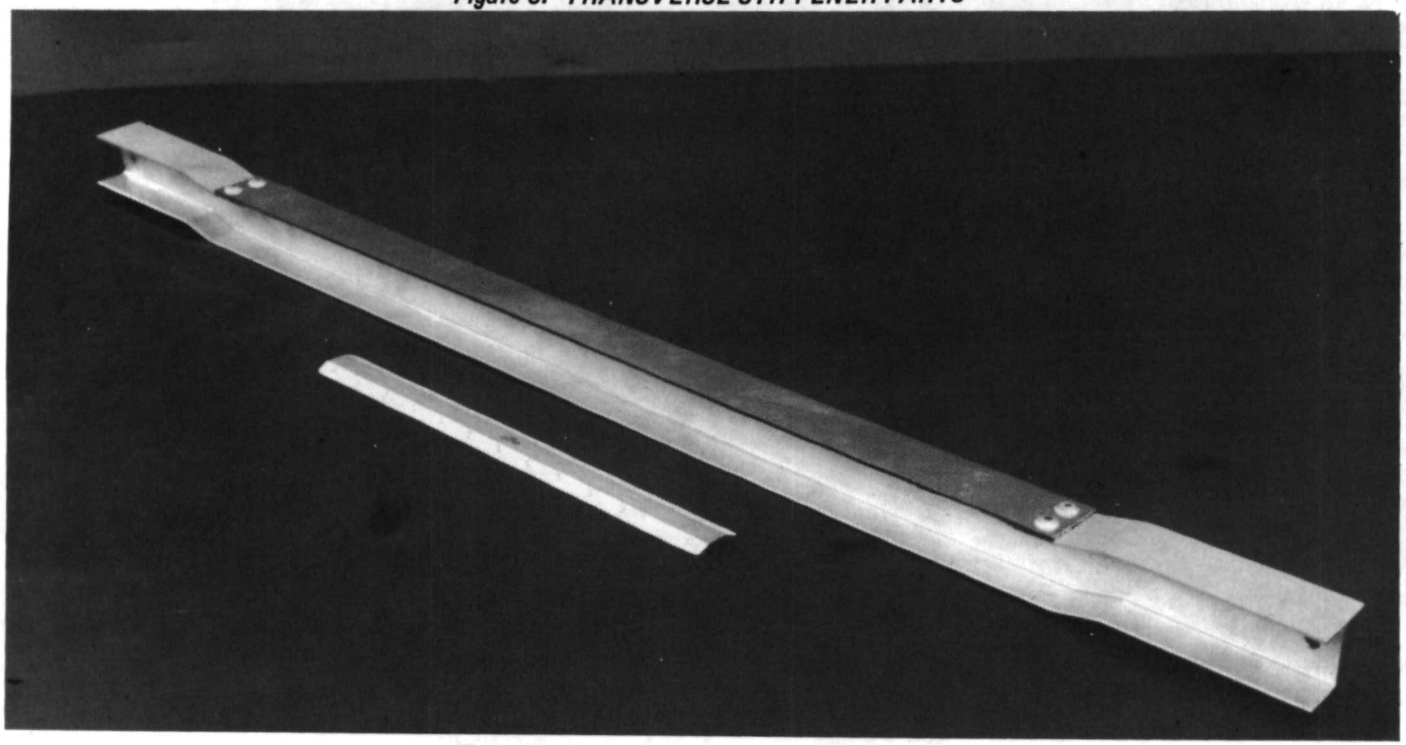

Figure 9: ***TRANSVERSE STIFFENER ASSEMBLY***

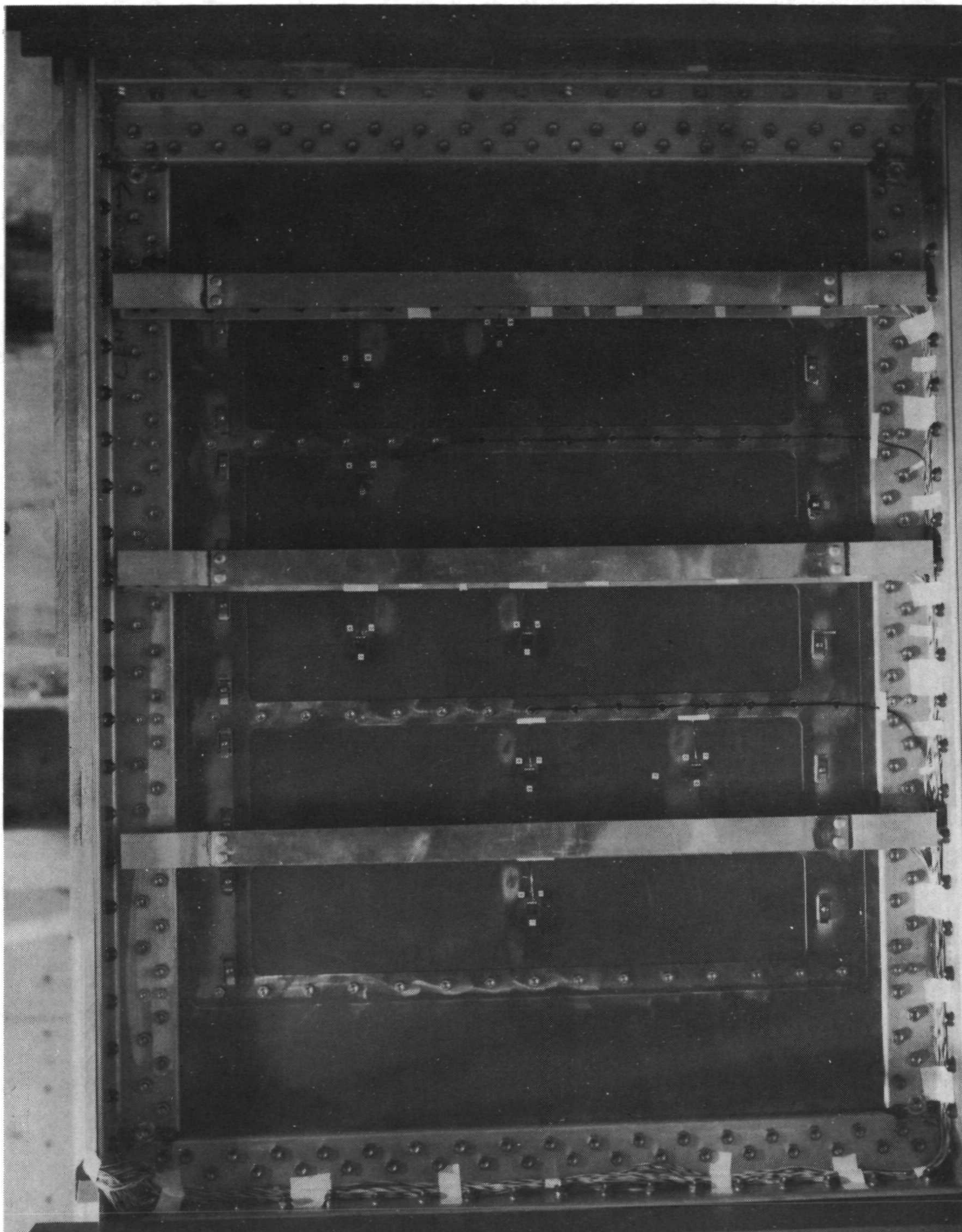

Figure 10: TEST WEB 1 ASSEMBLY

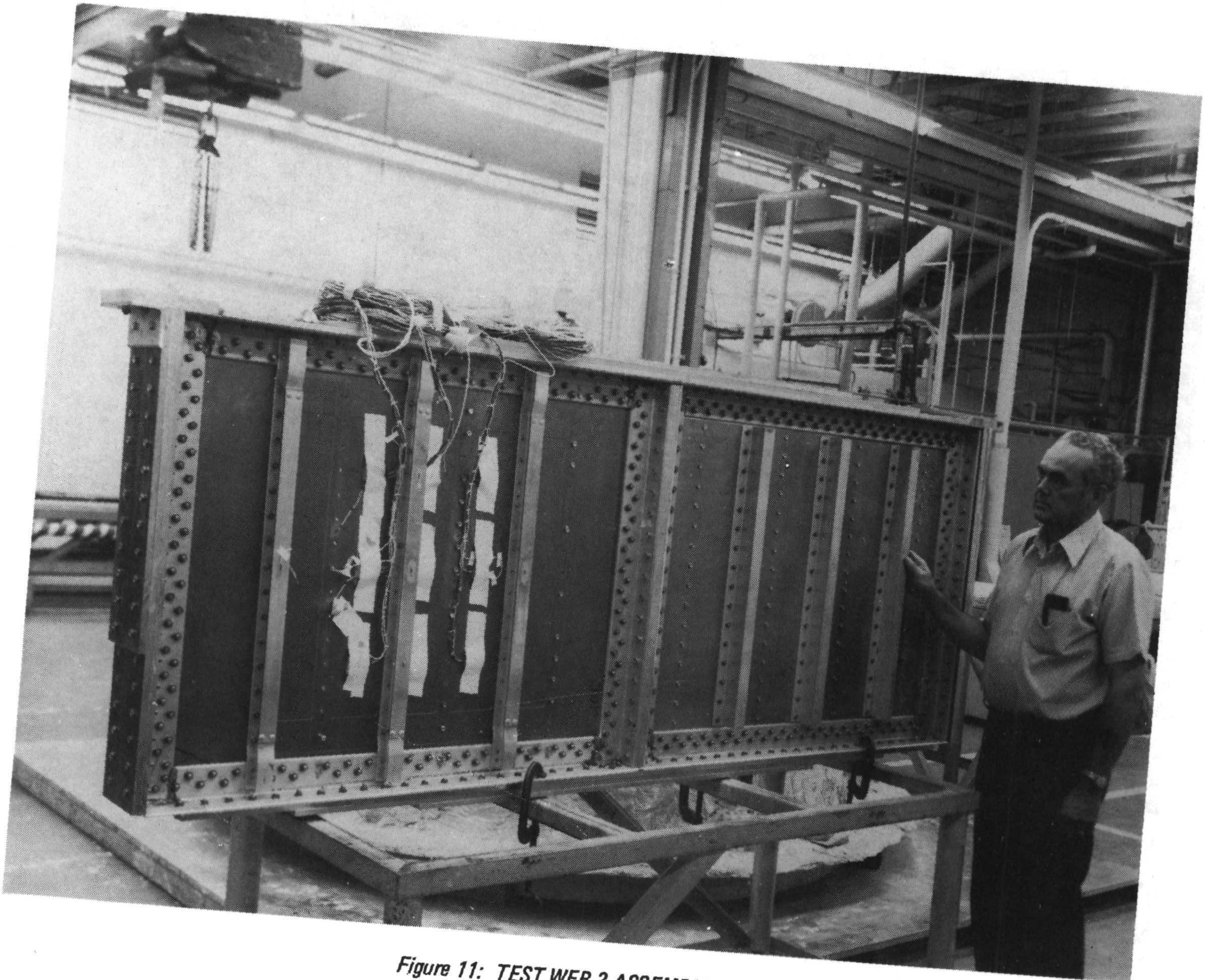

Figure 11: TEST WEB 2 ASSEMBLY

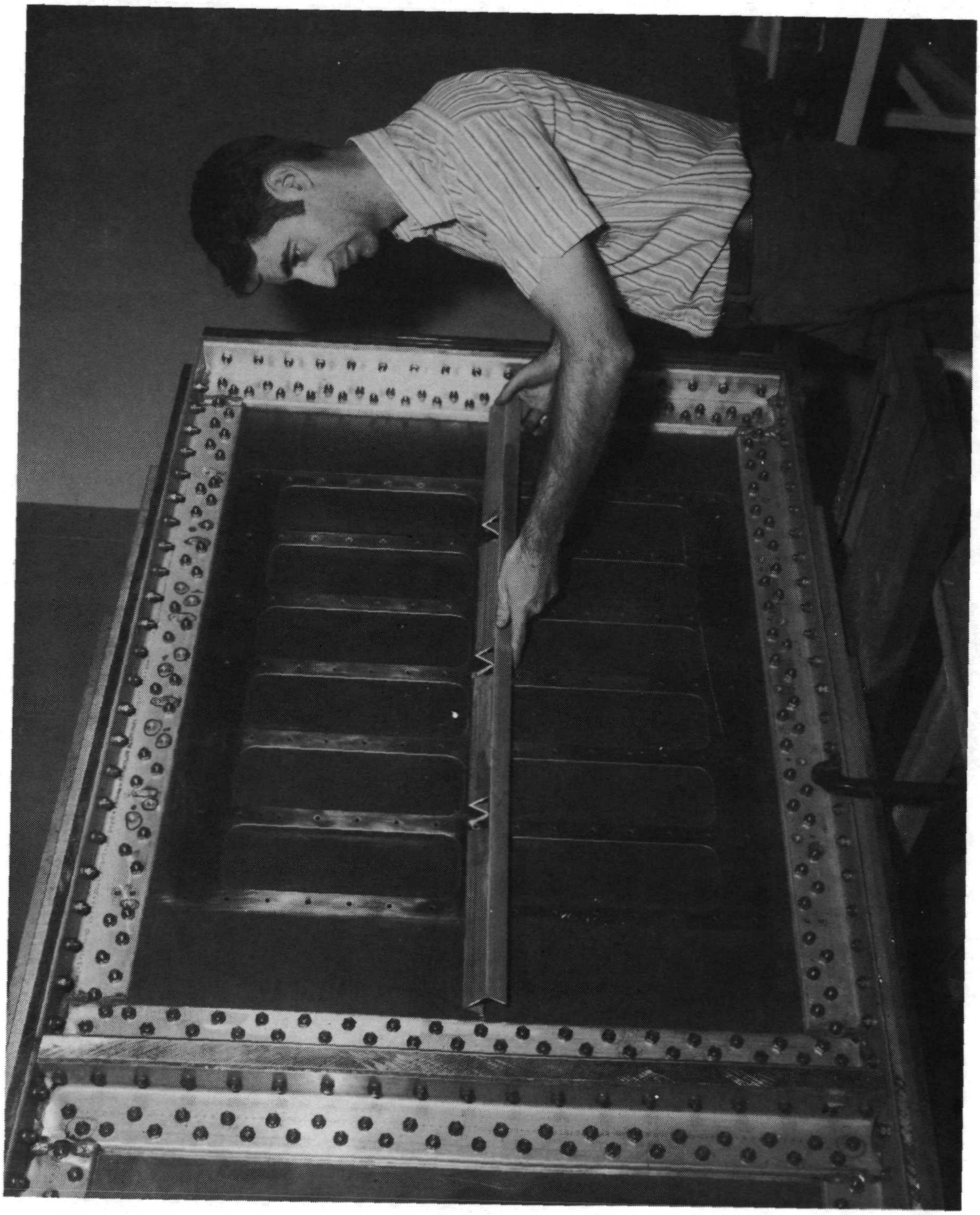

Figure 12: TEST WEB 3 SUBASSEMBLY

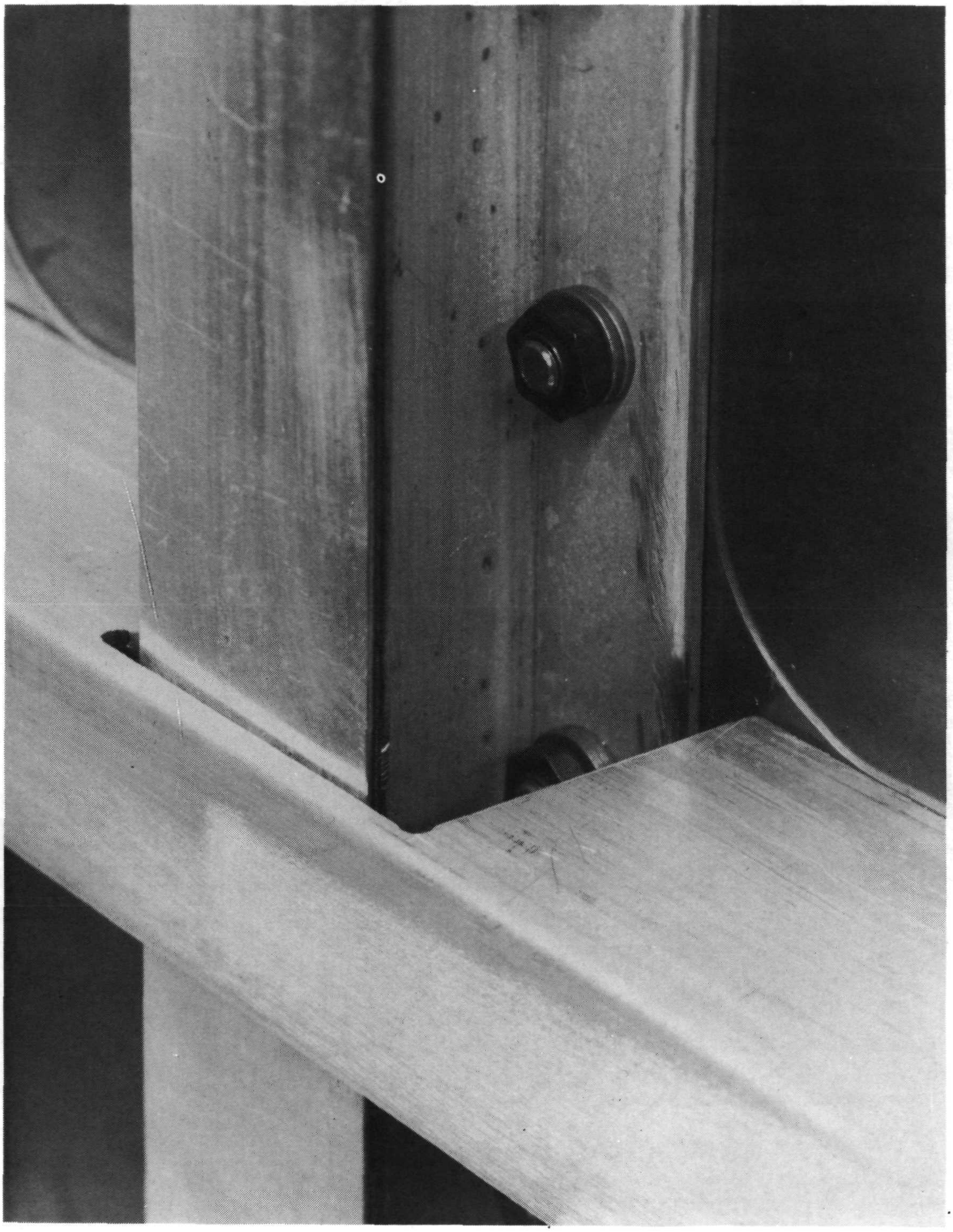

Figure 13: TEST WEB 3 LONGITUDINAL/TRANSVERSE STIFFENER CROSS-OVER DETAILS

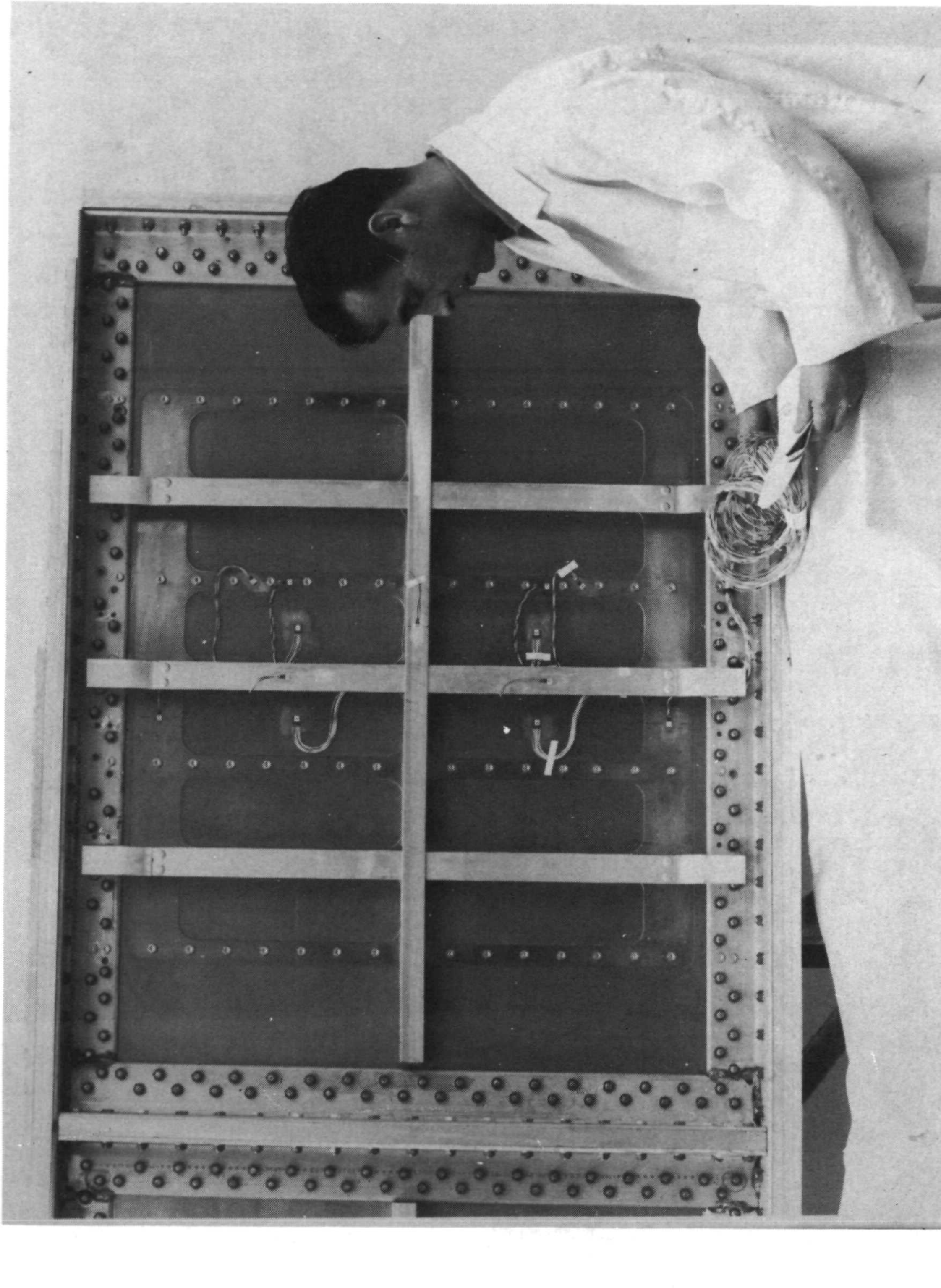

Figure 14: TEST WEB 3 ASSEMBLY

ADVANCED COMPOSITE	AVCO RIGIDITE 5505/4 BORON/EPOXY PREPREG TAPE
WEB LAMINATE ADHESIVE PLIES	NARMCO METLBOND 329
WEB LAMINATE METAL PARTS	6 Al-4V M.A. TITANIUM
TITANIUM BOND SURFACE PREPARATION	FACE SHEETS–PHOSPHATE FLOURIDE COATING PROCESS STEP-LAP DETAILS–VACU-BLAST & SILANE RINSE ALL PARTS–3M EC 2333 PRIMER
METAL STIFFENER PARTS	7075-T6 ALUMINUM (EXTRUSIONS FORMED IN THE 0 CONDITION)
STIFFENER ADHESIVE PLIES	MODERATE TEMPERATURE CURING EPOXY BOEING MATERIAL SPECIFICATION BMS 5-51 FOR LOW STRESSED STIFFENER PARTS ASSEMBLY

Figure 15: TEST WEB COMPONENT MATERIALS

Detailed test web component designs and material specifications are given in References [2] and [3]. Reference [2] presents the test beam framework detailed design and test web component manufacturing plans. Dimensions of the test web details needed for structural analysis are given in Section 6.3 of this report.

3.2 TEST WEB MASS SUMMARY

The test web component masses are summarized in Figure 16. The masses are calculated based on average measured material thicknesses (after bonding) and in some cases are actual masses. In the case of the third test web, the mass of B/E material is only 14% of the total web assembly mass of 59.1 lb (26.9 kg). The masses of the test webs are considered to be in excess of flight mass because of the use of "full stock sheet cladding thickness" at the edges of the web laminate. The use of the "reinforced cladding thickness" instead of the full stock sheet thickness is desirable for flight hardware and would reduce the total test web 3 mass to 56.0 lb (25.5 kg).

Item	TEST WEB COMPONENTS					
	1		2		3	
	Lb	kg	Lb	kg	Lb	kg
B/E Subassembly						
Titanium step-lap frame	3.95	1.79	3.95	1.79	3.95	1.79
Boron/epoxy	4.05	1.84	4.05	1.84	4.05	1.84
Adhesive	0.72	0.33	0.72	0.33	0.65	0.29
Calculated Total	8.72	3.96	8.72	3.96	8.65	3.92
Actual Total	(9.08)	(4.12)				
Web Laminate						
B/E subassemblies (2)	17.44	7.91	17.44	7.91	17.30	7.85
Adhesive	3.36	1.52	4.48	2.03	3.08	1.40
Titanium cladding skins	25.16	11.41	25.16	11.41	25.70	11.66
Calculated Total	45.96	20.85	47.08	21.36	46.08	20.90
Actual Total	(45.4)	(20.6)	(47.7)	(21.6)	(46.7)	(21.2)
Transverse stiffener						
Aluminum J-section	0.99	0.45	1.76	0.80	1.37	0.62
Titanium step-lap details	0.02	0.01	0.02	0.01	0.02	0.01
B/E reinforcement	0.14	0.06	0.14	0.06	0.14	0.06
Adhesive	0.02	0.01	0.02	0.01	0.02	0.01
Aluminum flange cladding skin	0.06	0.03	0.06	0.03	0.06	0.03
Calculated Total	1.23	0.56	2.00	0.91	1.61	0.73
Actual Total			(1.99)	(0.90)	(1.83)	(0.83)
Longitudinal stiffener (aluminum)						
Calculated Total	–	–	–	–	1.79	0.81
Calculated Web Assembly Mass	53.34	24.20	59.08	26.80	59.14	26.83

Figure 16: Test Web Assembly Masses (Fasteners Neglected)

4.0 COMPONENT TEST PROGRAM

The shear web components were tested at room temperature with the loadings listed in Figure 17. Test webs 1 and 3 were tested to failure and test web 2 was tested as a low-cycle fatigue test component. The second test was terminated in the 411th loading when strain gage data indicated that proportional limit strain was reached in the titanium cladding of the web laminate. This web was then examined for fatigue damage and later shipped to NASA/Langley.

The test webs were instrumented to record panel buckling displacements, strains, vertical and lateral deflections and acoustic emissions. A summary of the test instrumentation used in the first test is given in the test plan contained in the Phase I Report [1]; the instrumentation used in the second and third tests was essentially the same as in the first test.

The general test set-up is shown in Figures 18 and 19. The test beam was laterally supported at the ends and at the center where the loading was applied. Rollers were used to provide simple supports at the beam ends.

The test web buckling responses were monitored by the Moire fringe technique [4]. Equipment used to acquire Moire fringe data appears in front of the test beam in Figures 18 and 19 and is described in Reference [3]. A light source (the box with focusing lens) directed a strong light beam to a mirror located on the floor which reflected the beam to a mirror mounted on the glass Moire grid panes mounted on the test web component. A camera was positioned in front of the web to record the Moire fringe patterns that appeared during testing.

TEST WEB 1 STATIC STRENGTH TEST		TEST WEB 2 LOW-CYCLE FATIGUE TEST				TEST WEB 3 STATIC STRENGTH TEST	
1.	250,000 LB (1.11 MN)	1.	200,000 LB (.89 MN)	407.	450,000 (2.00)	1.	200,000 LB (.89 MN)
2. to 102.	100 CYCLES TO 400,000 (1.78)	2.	400,000 (1.78)	408.	425,000 (1.89)	2.	575,000 FAILURE (2.56)
103.	540,000 FAILURE (2.40)	3.	400,000 (1.78)	409.	490,000 (2.18)		
		4. to 404.	400 CYCLES TO 400,000 (1.78)	410.	490,000 (2.18)		
		405.	436,000 (1.94)	411.	530,000 (2.36)		
		406.	449,000 (2.00)		NO FAILURE		

Figure 17: TEST BEAM LOADINGS

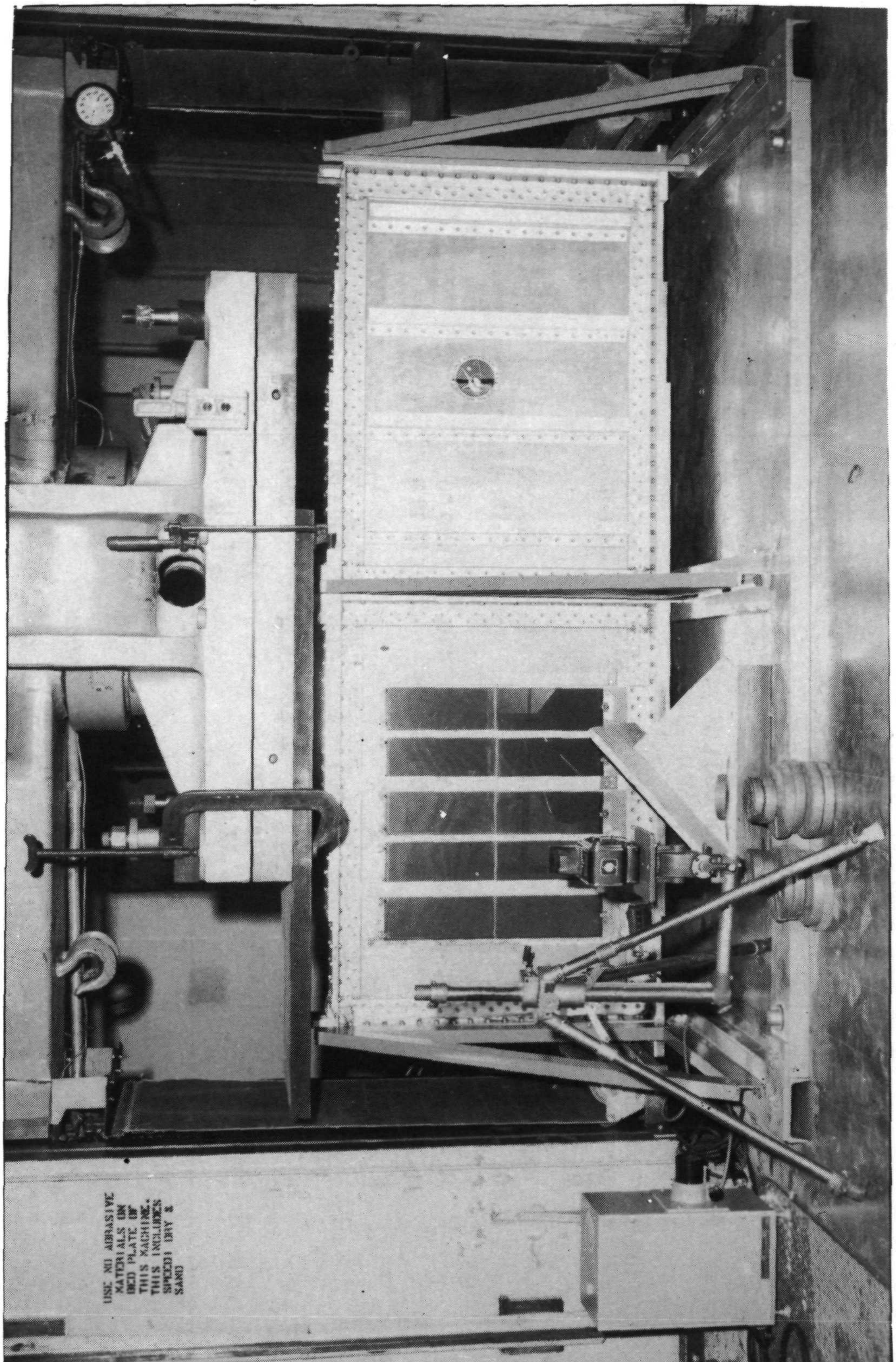

Figure 18: SHEAR WEB COMPONENT TEST SET-UP

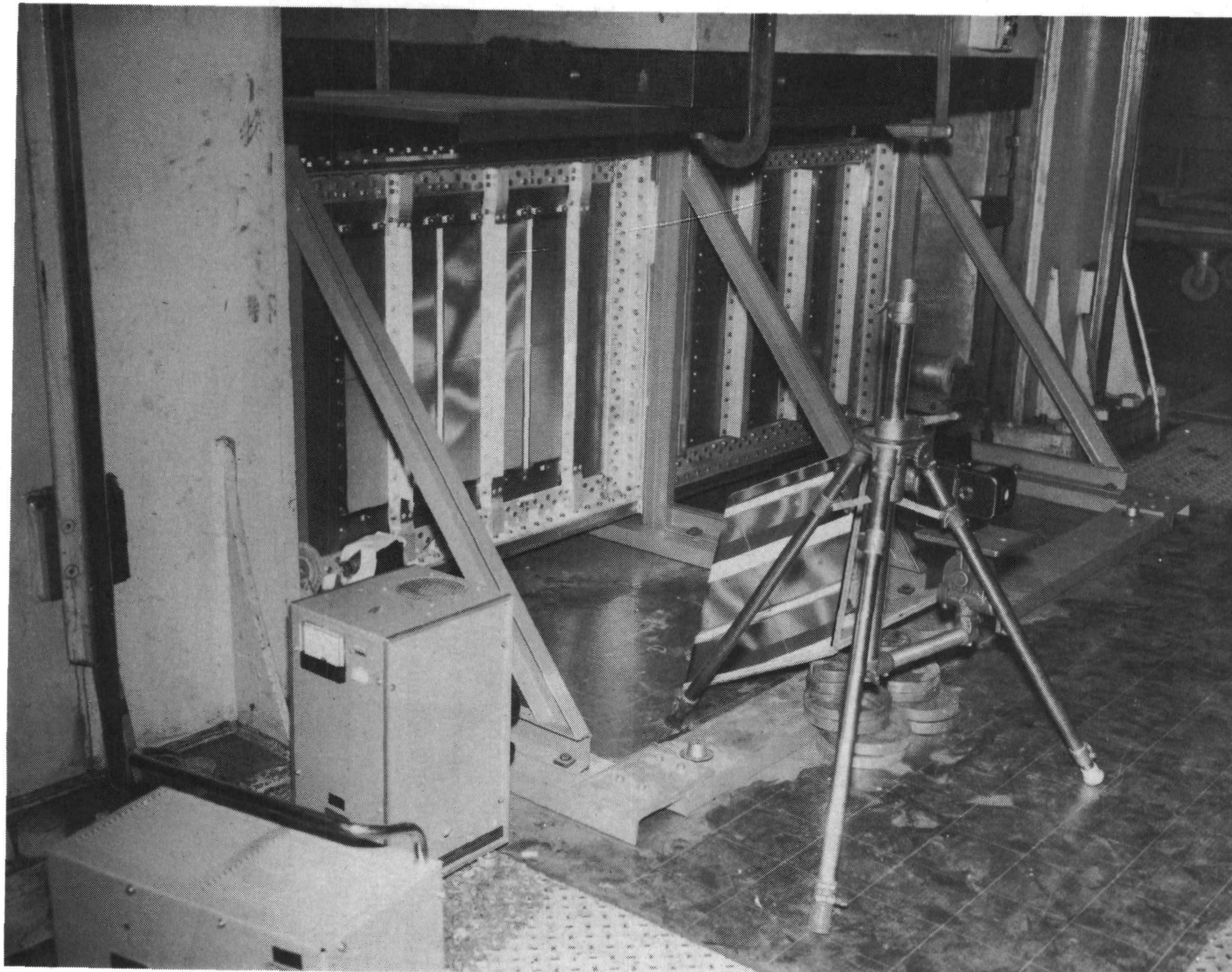

Figure 19: MOIRE FRINGE INSTRUMENTATION SET-UP

5.0 TEST DATA SUMMARY

The shear web component test data are summarized in this section with respect to observed deflections, and strains and failure characteristics. The test data are presented in greater detail in Reference [3].

5.1 LOAD/DEFLECTION DATA

The load/center deflection responses are given in Figure 20. In comparison with the initial load/deflection responses, load/deflection stiffnesses predicted by finite element analysis of the test webs using the NASTRAN code are within 5% of the actual test values [3]. The non-linear response is due to slippage in the test beam assembly and web buckling deflections. The stepped response of test web 3 is a result of time-dependent lateral web deflections which occurred in load holding periods during the final loading; this response was investigated [3] and was found to be non-critical for the application assumed in this program. The time-dependent response was concluded to be primarily due to inter-laminar shear creep in the polymeric parts of the web laminate and, to limited extent, to slippage at stiffener interfaces.

5.2 STRAIN DATA

Principal strain data from strain gages at or near critical panel deflection areas are shown in Figures 21 to 23. The strain data reflects the increase in buckling resistance obtained in going from test web 1 to 3. Web laminate bending (buckling) deformation is indicated in the plots by a deviation of the respective strains from the back-to-back gages. The influence of initial imperfections is apparent in the data for test web 1 (which had the highest initial flatness imperfection) where the web out-of-plane bending response initiated at low load. Test web 3 was relatively buckle resistant until near the failure load.

5.3 MOIRE FRINGE PATTERN DATA

The Moire fringe (interference) pattern photographs at selected load levels are presented in Figures 24 to 26 for test web 2 and Figures 27 to 31 for test web 3. The Moire fringe instrumentation parameters for each test are defined in Reference [3]. The essential parameter for structural analysis is the fringe order calibration defined as the panel surface displacement per one fringe order. Each fringe order appears in the patterns as a dark

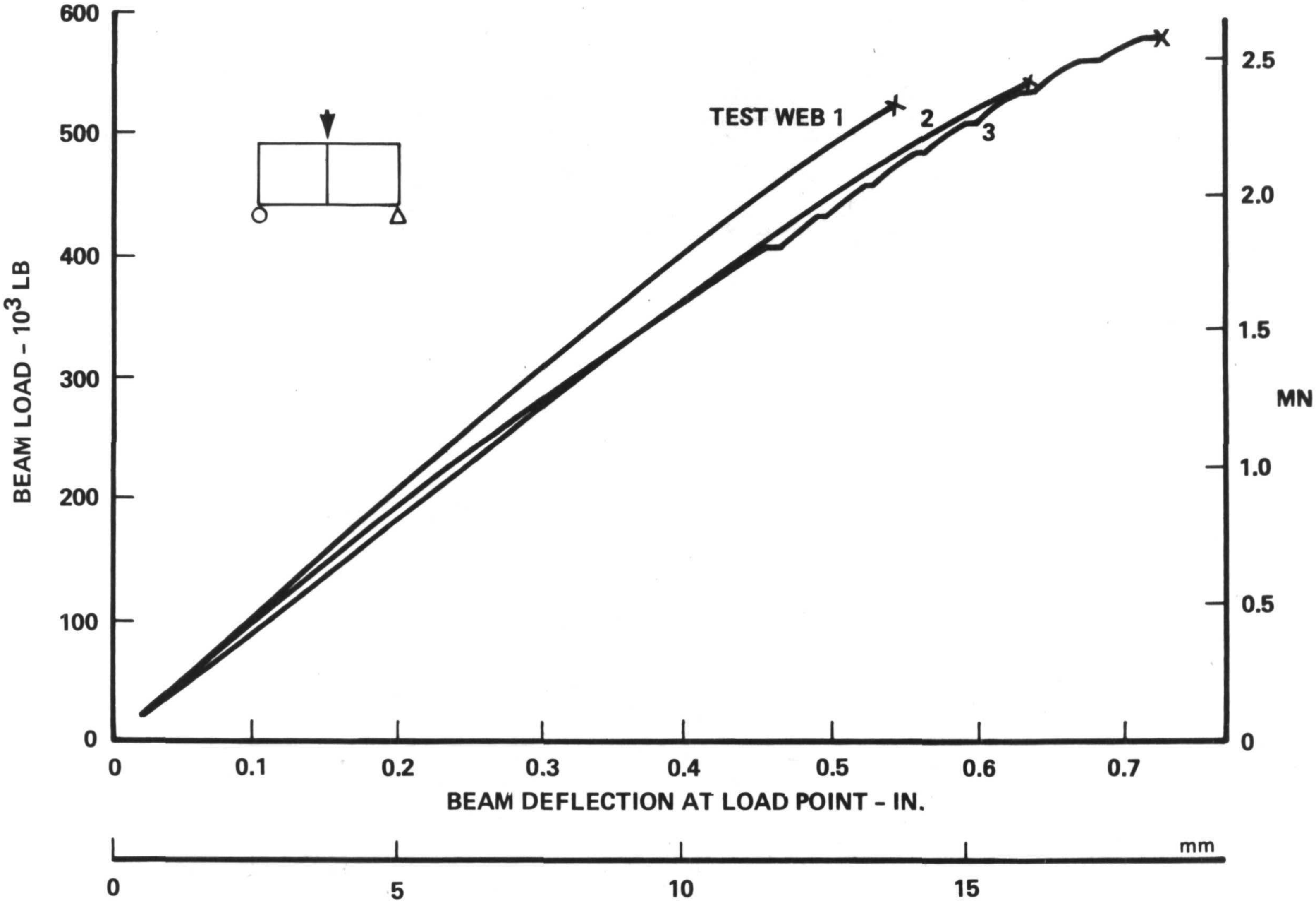

Figure 20: LOAD/DEFLECTION RESPONSES

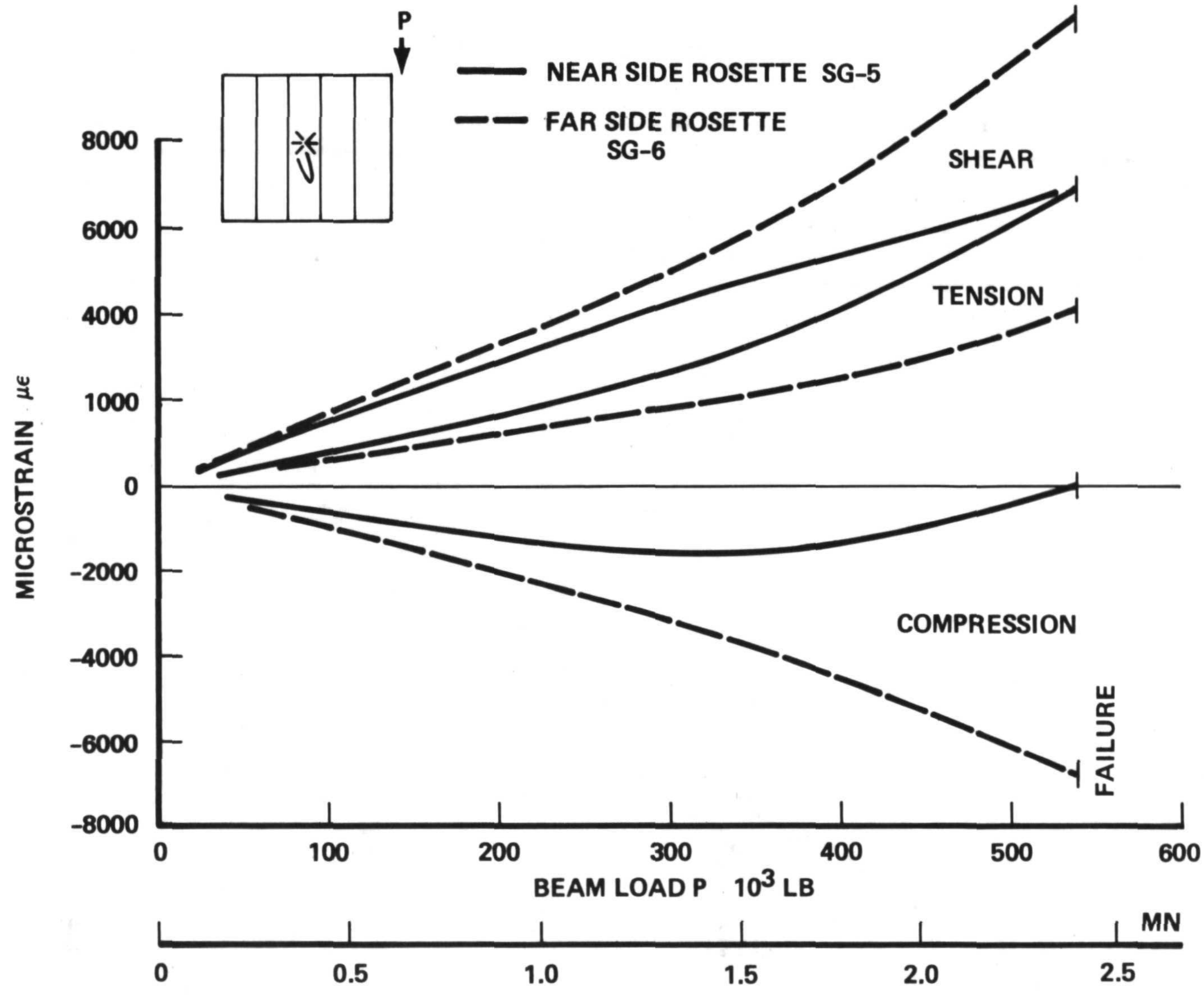

Figure 21: TEST WEB 1 PRINCIPAL SURFACE STRAINS IN CRITICAL BUCKLE AREA

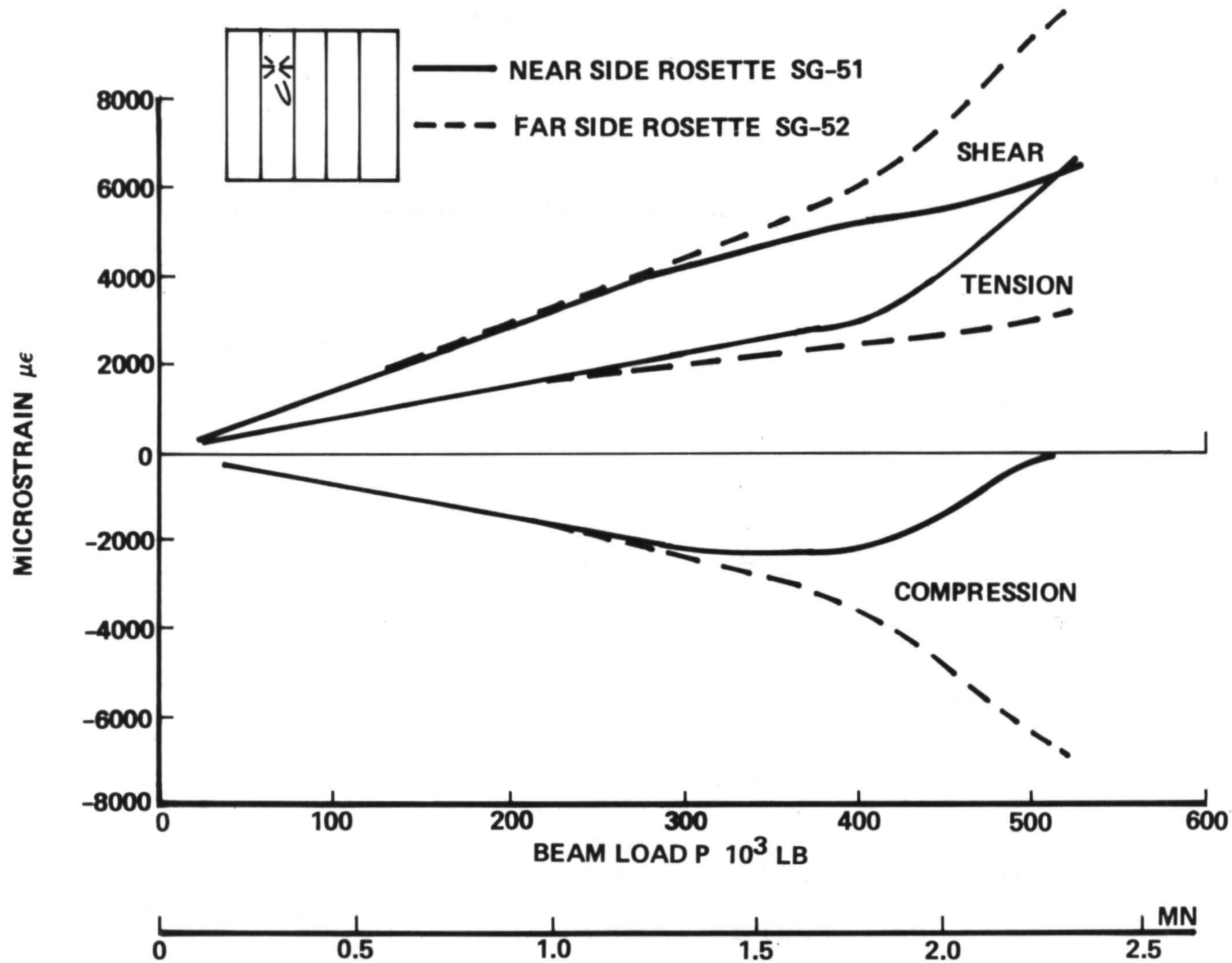

Figure 22: TEST WEB 2 PRINCIPAL SURFACE STRAINS IN CRITICAL BUCKLE AREA

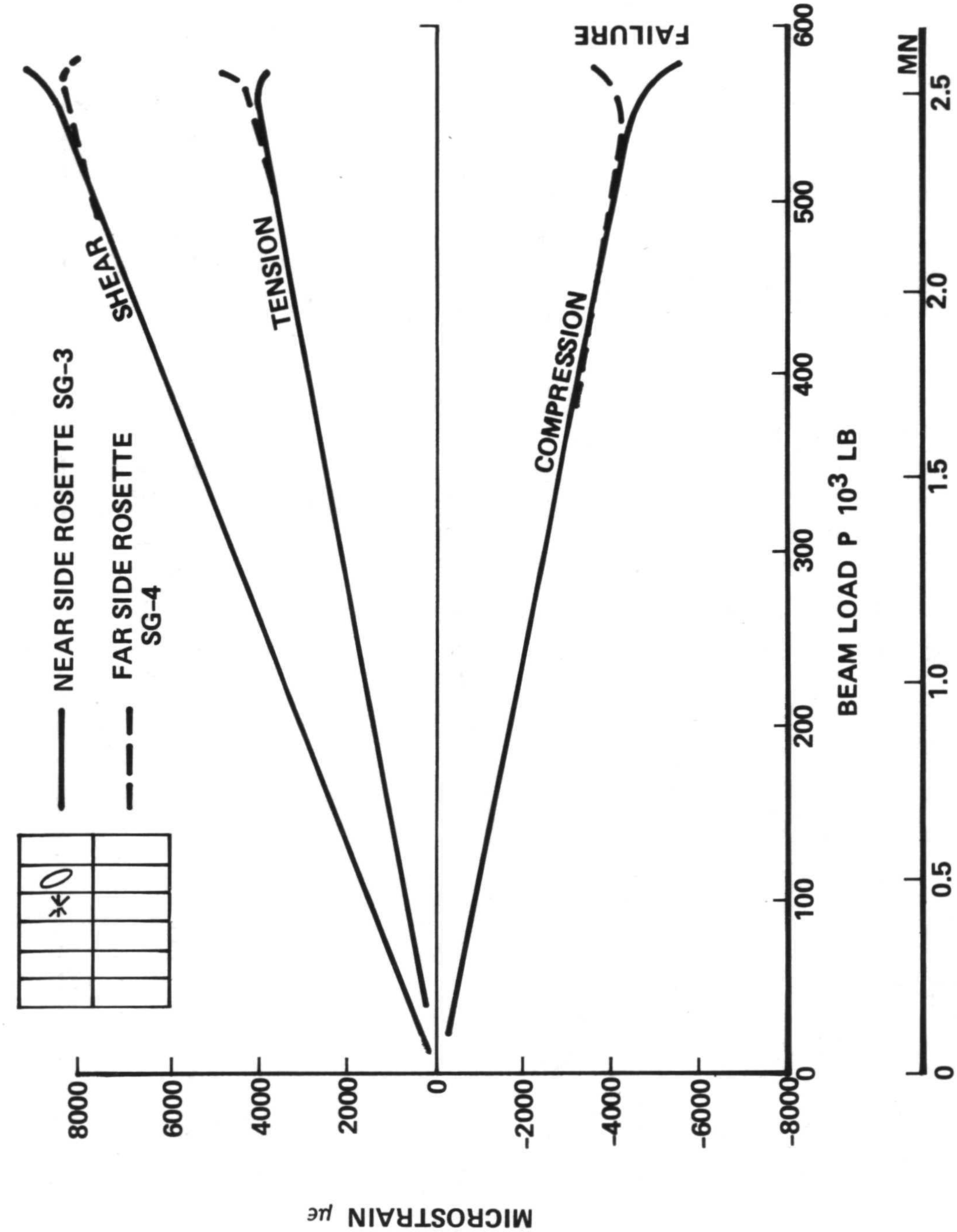

Figure 23: TEST WEB 3 PRINCIPAL SURFACE STRAINS NEAR CRITICAL BUCKLE AREA

Figure 24: *TEST WEB 2 MOIRE FRINGE PATTERN AT ZERO LOAD AFTER LOAD CYCLING*

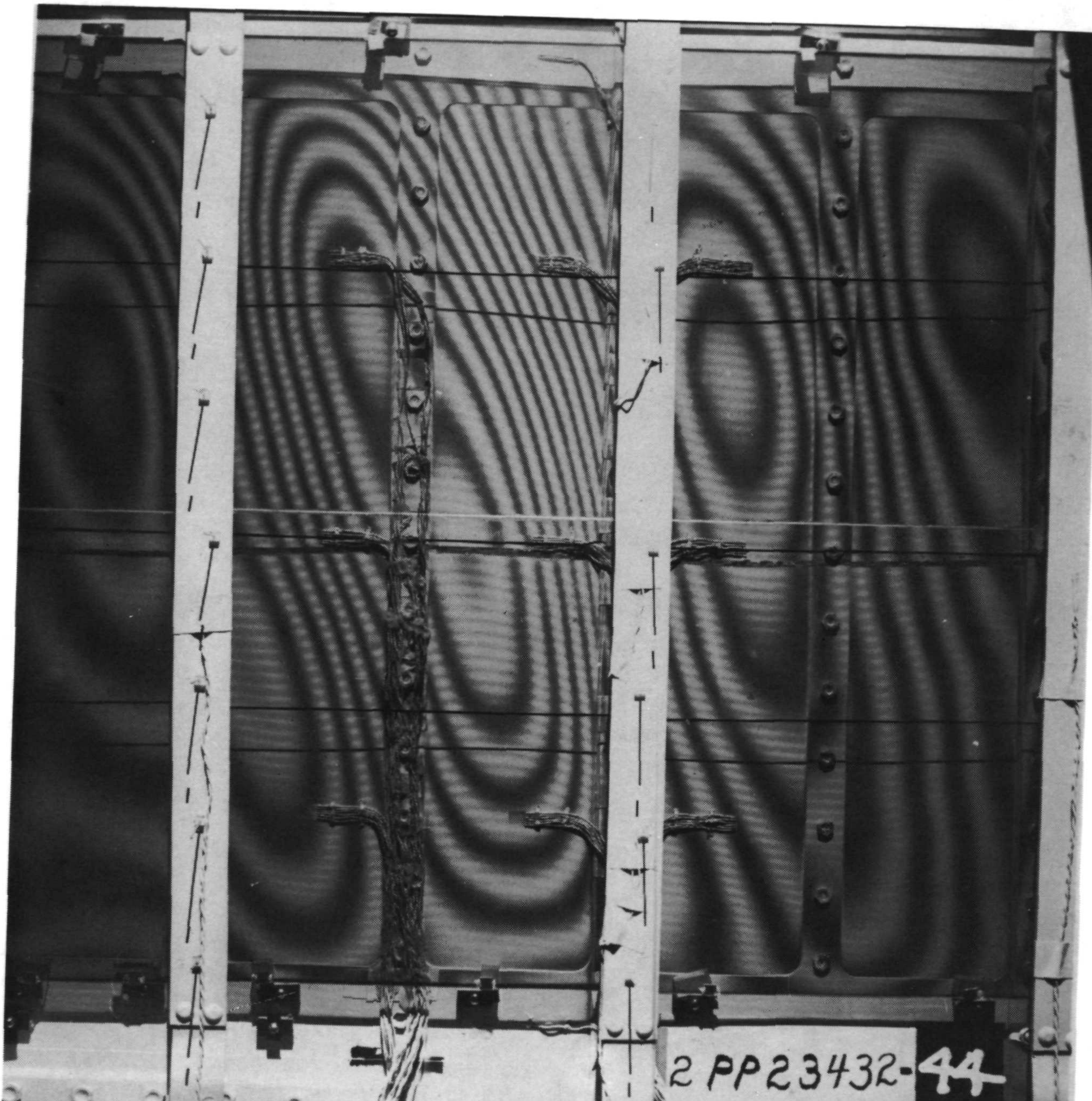

Figure 25: TEST WEB 2 AT 400,000 LB (1.78 MN) AFTER LOAD CYCLING

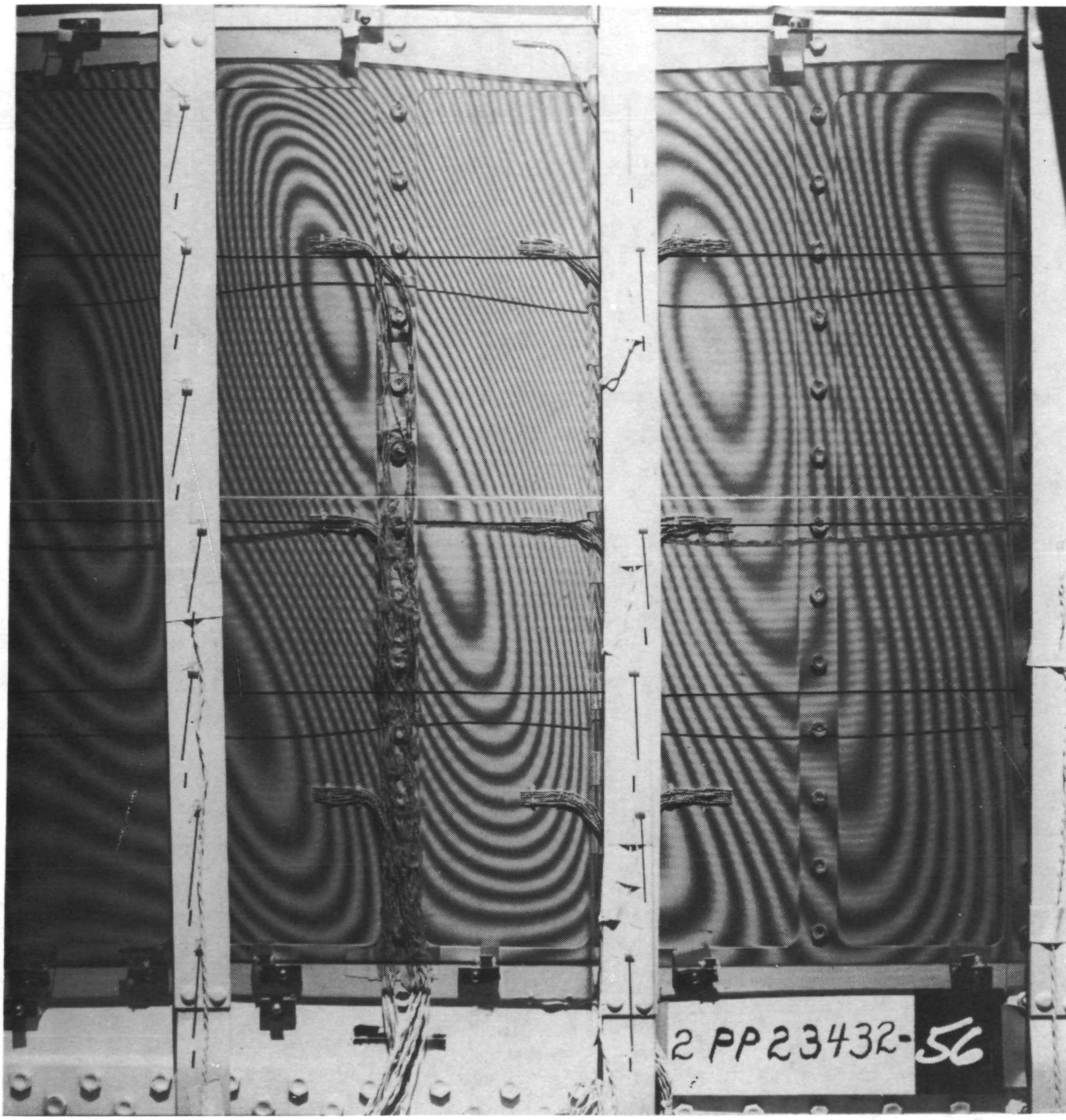

Figure 26: TEST WEB 2 AT 530,000 LB (2.36 MN) AFTER LOAD CYCLING

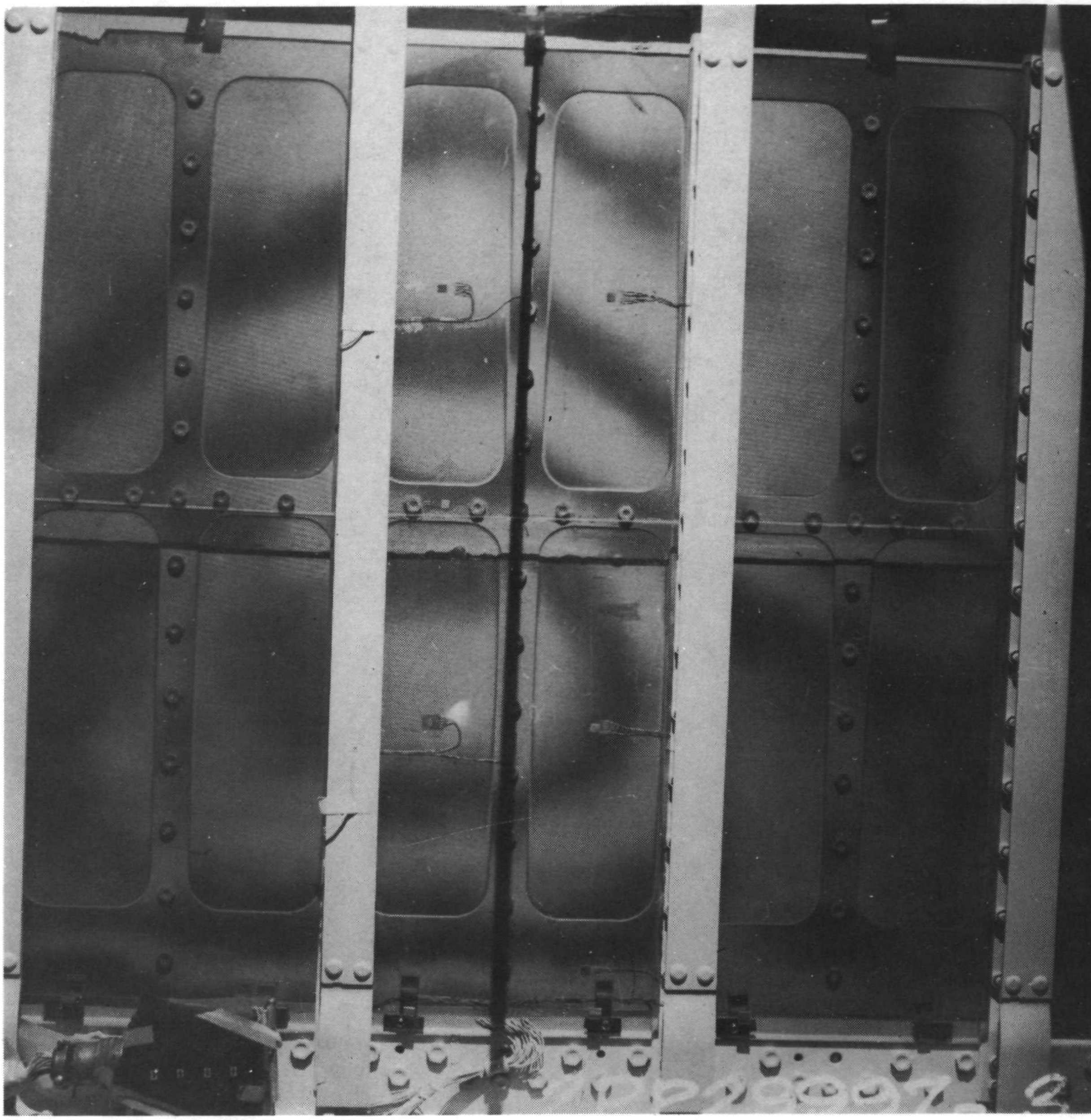

Figure 27: TEST WEB 3 MOIRE FRINGE PATTERN AT ZERO LOAD

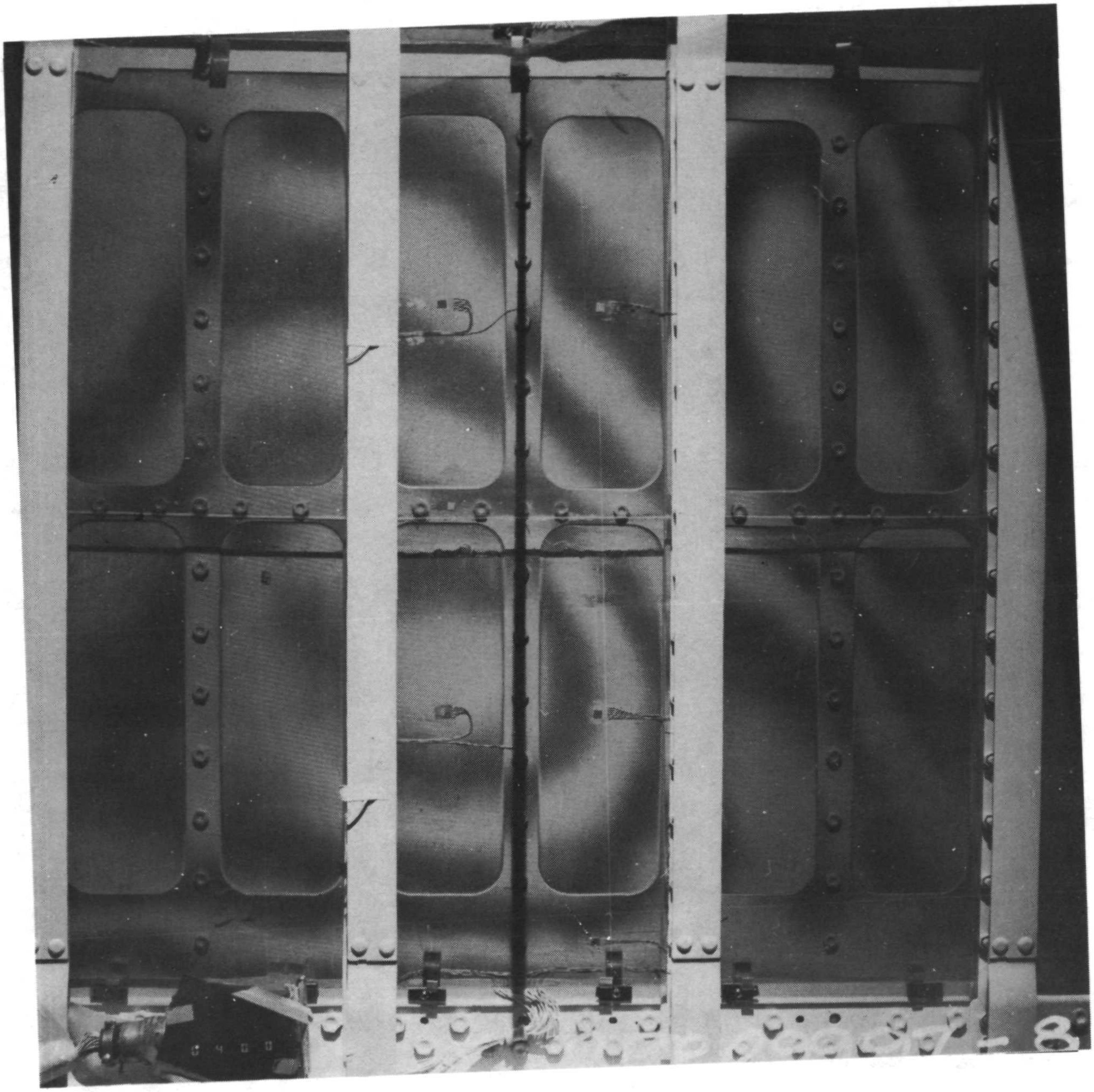

Figure 28: TEST WEB 3 AT 400,000 LB (1.78 MN)

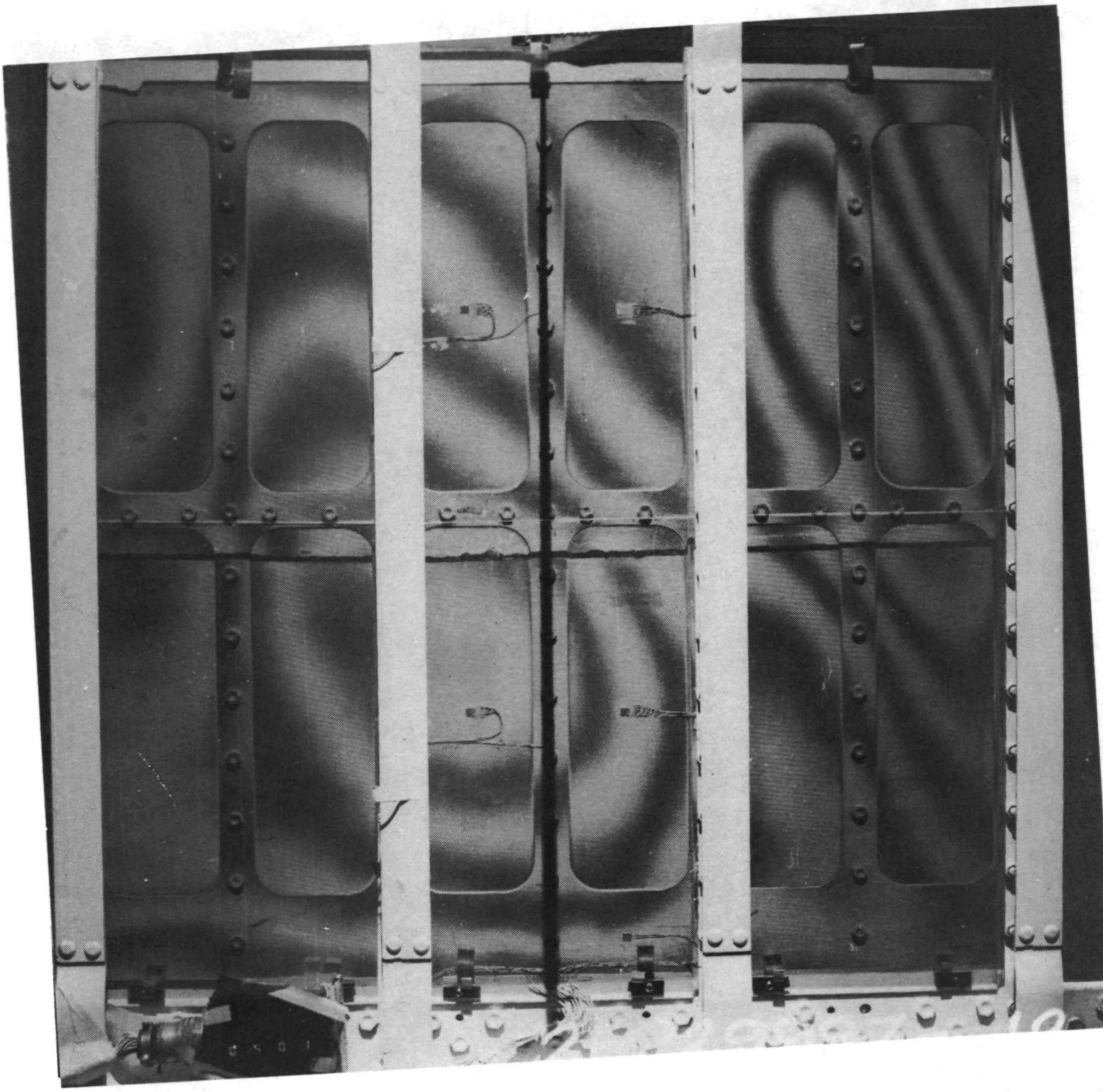

Figure 29: TEST WEB 3 AT 500,000 LB (2.22 MN)

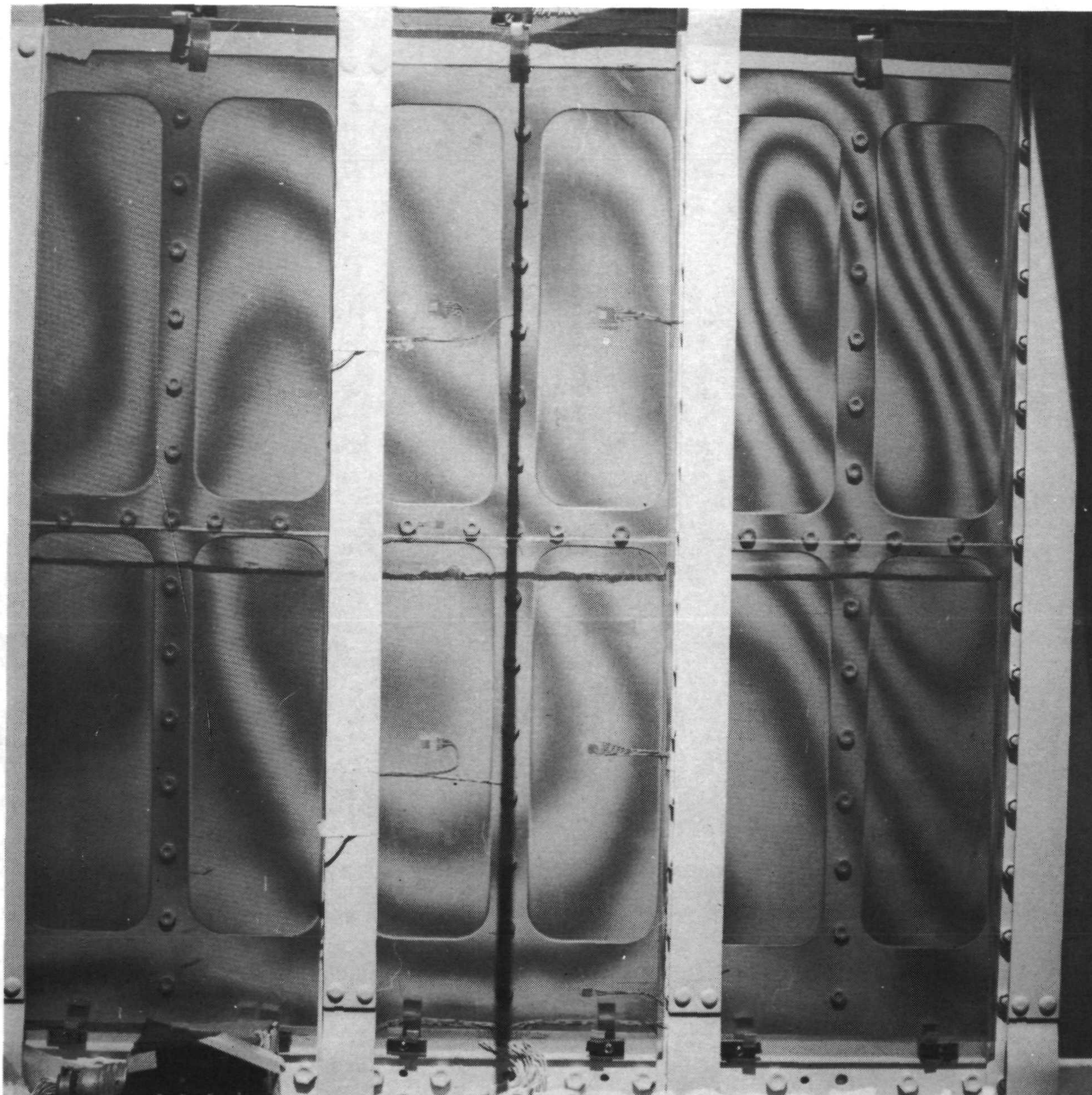

Figure 30: TEST WEB 3 AT 550,000 LB (2.45 MN)

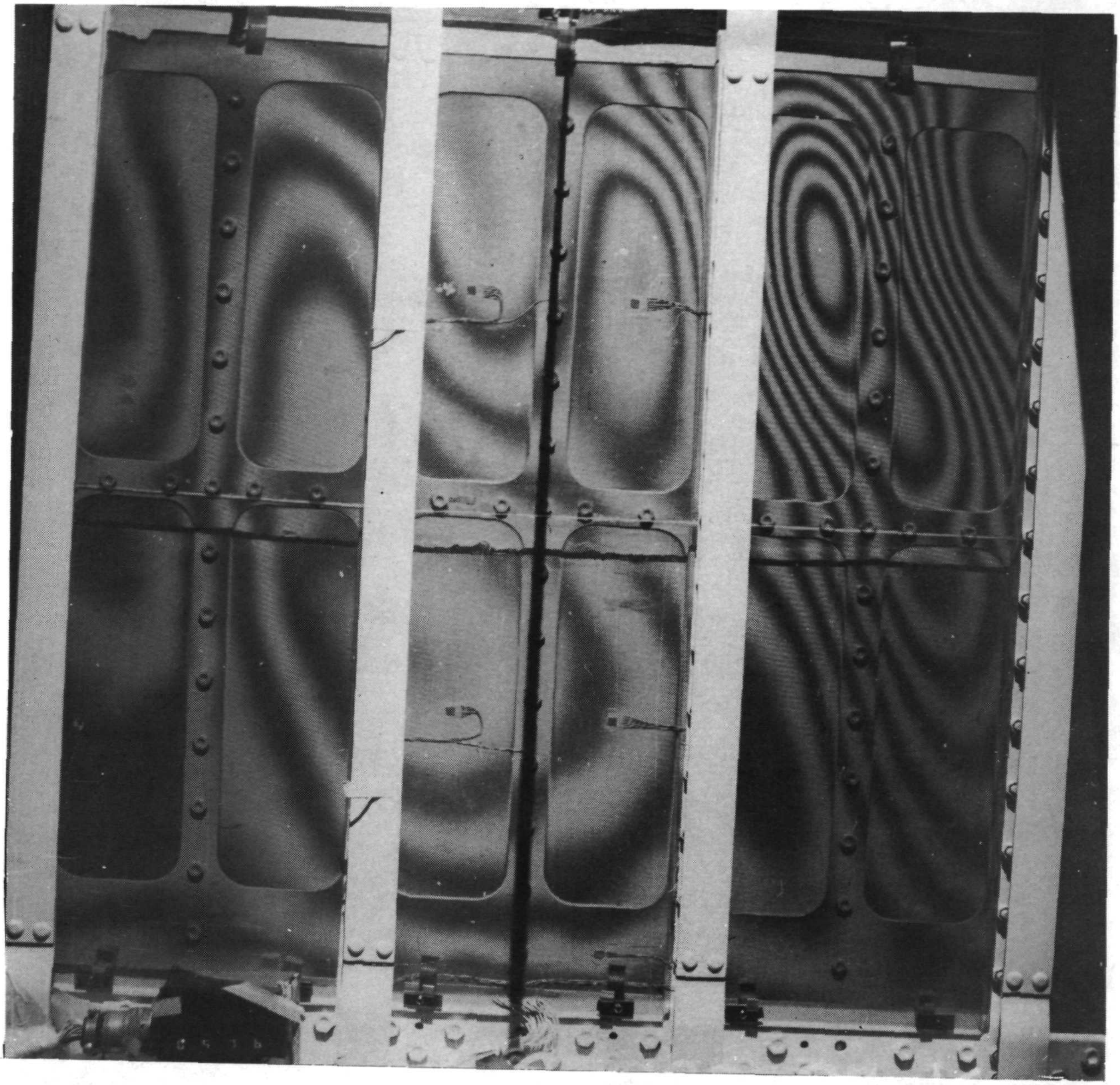

Figure 31: TEST WEB 3 AT 575,000 LB (2.56 MN)

topographic line. The respective fringe order calibration factors for test webs 2 and 3 are 0.01875 inch (0.476 mm) and 0.01730 inch (0.439 mm).

Some aspects of the Moire fringe instrumentation can be pointed out in the pattern photographs. The attachment points of the glass grid panes can be seen in the photographs; a three point mounting arrangement was used for each pane to isolate the pane from the central web centerline. Glued pane splices were used and they can be seen along the web centerline. The shadows from these splices are indicators of the buckle deflections. In the second test, horizontal tape stripes and short posts bonded to the stiffeners cast shadows which assist in defining the deflection state. The post shadows indicate stiffener rotation in terms of shadow movement from an initial reference mark.

The second test web is shown in Figure 24 at zero load after load cycling. Initial flatness imperfections were introduced in this web during final assembly and these imperfections grew very slightly during load cycling to about level of ±0.014 in. (0.356 mm) deviation from a mean flat surface. This growth in imperfection is attributed to slippage between the stiffeners and the web laminate (the fasteners were non-hole filling and were torqued to low level to avoid laminate crushing). At the cyclic load level of 400,000 lb (1.78 MN), the maximum prebuckling panel deflection is on the order of ±0.1 in. (2.54 mm) or about one-half laminate thickness. Coupled plate/stiffener pre and postbuckling is clearly displayed in Figures 25 and 26, respectively. Significant stiffener rotations are indicated by movement of the post shadows.

Test web 3 displayed high stability during loading until about 500,000 lb (2.22 MN) when buckle-like deformation initiated in the upper parts of the two right most panels (Figure 29). As loading proceeded to failure, the critical prebuckling deformation developed in the second right panel with evidence of coupled plate/stiffener response. The estimated initial imperfection in this area is ±0.003 in. (0.076 mm) based on measurements and the initial Moire fringe data. There was a slight thickness underrun of the web laminate in the critical buckle area [2] and this, along with the proximity to the loading area, is believed to have triggered the buckling response.

Non-linear strains were recorded on test web 3 by a strain gage on the reinforced laminate area just above the third panel from the right. These strains and the Moire fringe patterns shown in Figure 34 indicate that buckling type deformations were extending into areas near the chord angles; e.g., the effective panel height was greater than the nominal laminate panel height.

5.4 ACOUSTIC EMISSION DATA

High and low frequency acoustic emissions were recorded during the web component tests. Unlike the results obtained in tension element testing in Phase I [1], the web component emission data was difficult to interpret. Emissions having a signature like composite fracture did occur momentarily at failure. The test beam assembly was noisy during loading due to local slippages and the webs responded as microphones to background laboratory noise. These annoyances made analysis of the recorded emissions difficult but it is believed that damaging composite fracturing did not occur in any test except at the moment of failure.

5.5 POST-TEST INSPECTIONS

Inspections of the web components after testing revealed no areas where local design detail improvements would be necessary. The joint and reinforced laminate areas appeared to have functioned properly. Figure 32 shows the third web after failure. The "brittle" nature of failure of this type of construction is apparent in the figure. The fractures of the first and third webs appear to have originated in the buckled panel areas. Some fractures extended into the edge joint areas. The nature of damage in these tests indicated that failure did not initiate in the joint areas, based on failure mode studies of the element tests in Phase I [1].

Ultrasonic scans were made of the second test web before and after fatigue testing and the scan recordings indicated essentially no differences in the signatures except for those due to a change in sonic scan power level. Some edge delaminations were produced when the edge holes were drilled [2]; testing did not aggravate any of these delaminated areas. X-rays taken of the corners of the third test web indicate that the step-lap joint details performed satisfactorily. The B/E reinforced transverse stiffeners also appear to have functioned without premature failure in all testing.

Figure 32: TEST WEB 3 AFTER FAILURE (REAR SIDE)

6.0 TEST DATA ANALYSIS

6.1 FAILURE MODES ANALYSES

The shear web components responded to testing as summarized in Figure 33. Based on analysis of the strain and Moire fringe data, the first and third web components failed by composite fracturing in the critical laminate panel areas. The strains in the extreme B/E plies in the principal compression direction due to membrane and bending exceeded the assumed design allowable B/E strain of $6000\mu\epsilon$. The associated surface strains caused the titanium-cladding to slightly exceed the proportional limit for biaxial strain conditions.

6.2 FORCE/STRAIN ANALYSES

The force/strain (F/S) data plotting procedure was employed to define the linear bifurcation buckling loads of the test webs; these buckling loads are correlated with analytical predictions in the next section (Section 6.3). This procedure is also referred to as the force/stiffness technique [5]. Bifurcation buckling (sudden buckling) did not actually develop in the first and second webs because large deflection effects produced a smooth transition from prebuckling to postbuckling conditions. The use of the F/S technique allowed definition of the classical bifurcation buckling load in these tests. The F/S plots also served to define the bifurcation buckling loads in the third web test in which a postbuckled condition did not develop.

Figures 34 to 36 are the F/S plots for the web components that serve to define the respective bifurcation buckling loads. P/ϵ_B is plotted against P where P is the beam load and ϵ_B is the web laminate bending strain determined from the principal compression strain data recorded by strain gages closest to the largest panel buckling displacement area. The bifurcation buckling load is defined as the linear extrapolation of the prebuckling response to the load axis for the initial load condition. As shown by the F/S plots, the bifurcation buckling total beam loads are defined as:

Test Web 1	370,000 lb	(1.646 MN)
Test Web 2	425,000 lb	(1.89 MN)
Test Web 3	580,000 lb	(2.60 MN)

These test buckling loads are correlated with computed buckling loads in the next section. In defining the test buckling loads, F/S data for the initial load condition was used wherever

TEST WEB	MAXIMUM LOAD	COMMENTS
1	540,000 LB (2.4 MN)	• FAILED BY COMPOSITE FRACTURING IN POST-BUCKLED PANELS AT A 1.5 MAX. LOAD TO BIFURCATION BUCKLING LOAD RATIO
2	530,000 LB (2.36 MN)	• LOADED 400 CYCLES TO 400,000 LB (1.78 MN) WHICH PRODUCED 0.1 IN. (2.54 MN) MAXIMUM PANEL PRE-BUCKLING DEFLECTION • WEB WAS IN POST BUCKLED CONDITION AT MAXIMUM LOAD • NO APPARENT DAMAGE OCCURED
3	575,000 LB (2.56 MN)	• FAILED BY COMPOSITE FRACTURING AT HIGH PRE-BUCKLING PANEL STRAINS • FAILURE OCCURED WHILE HOLDING MAXIMUM LOAD (2.1 MINUTES) • EVIDENCE OF SMALL TIME-DEPENDENT LATERAL WEB DEFLECTION RESPONSE

Figure 33: SHEAR WEB COMPONENT TEST RESULTS SUMMARY

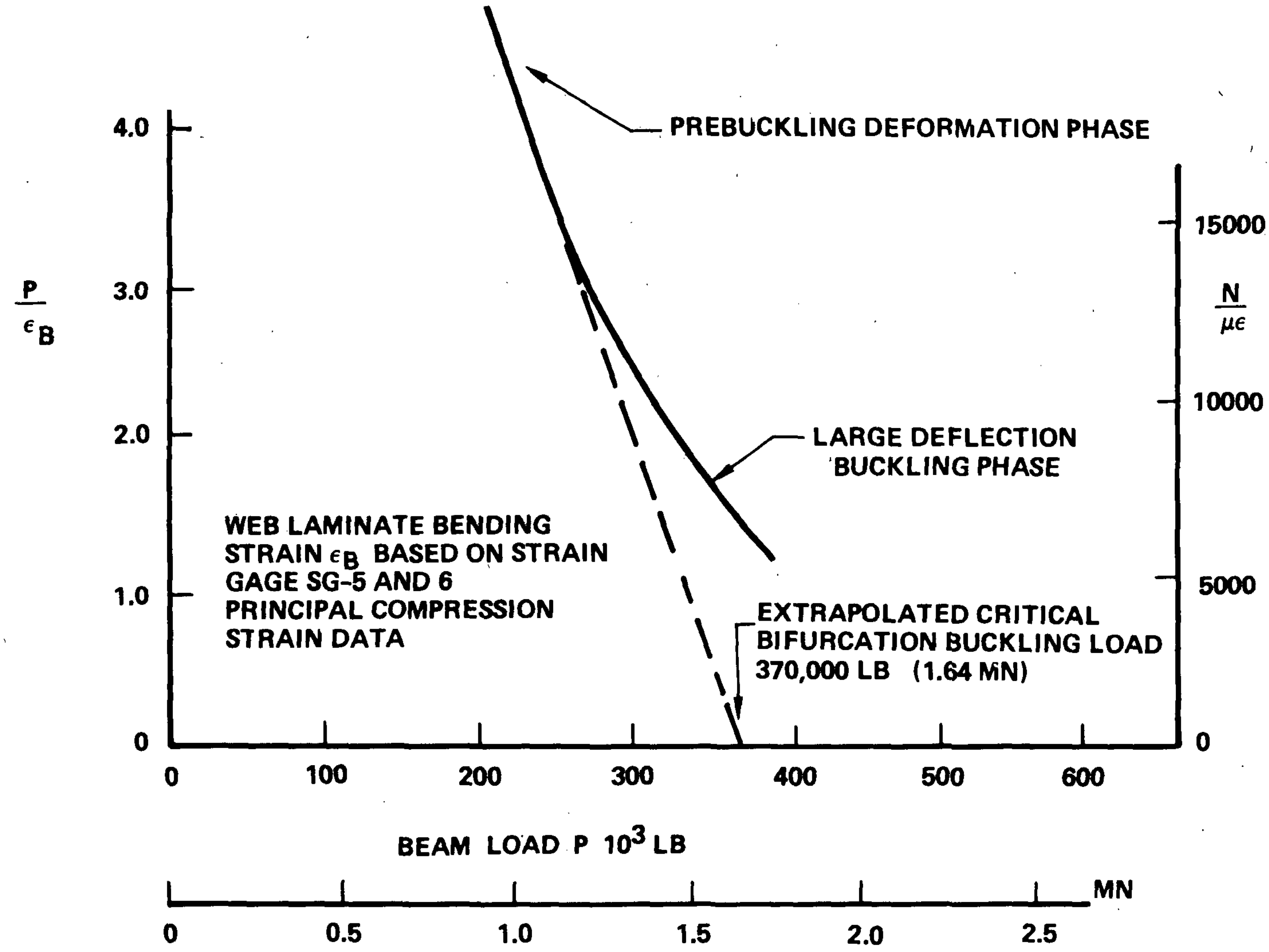

Figure 34: FORCE/STRAIN PLOT FOR TEST WEB 1 INITIAL LOADING

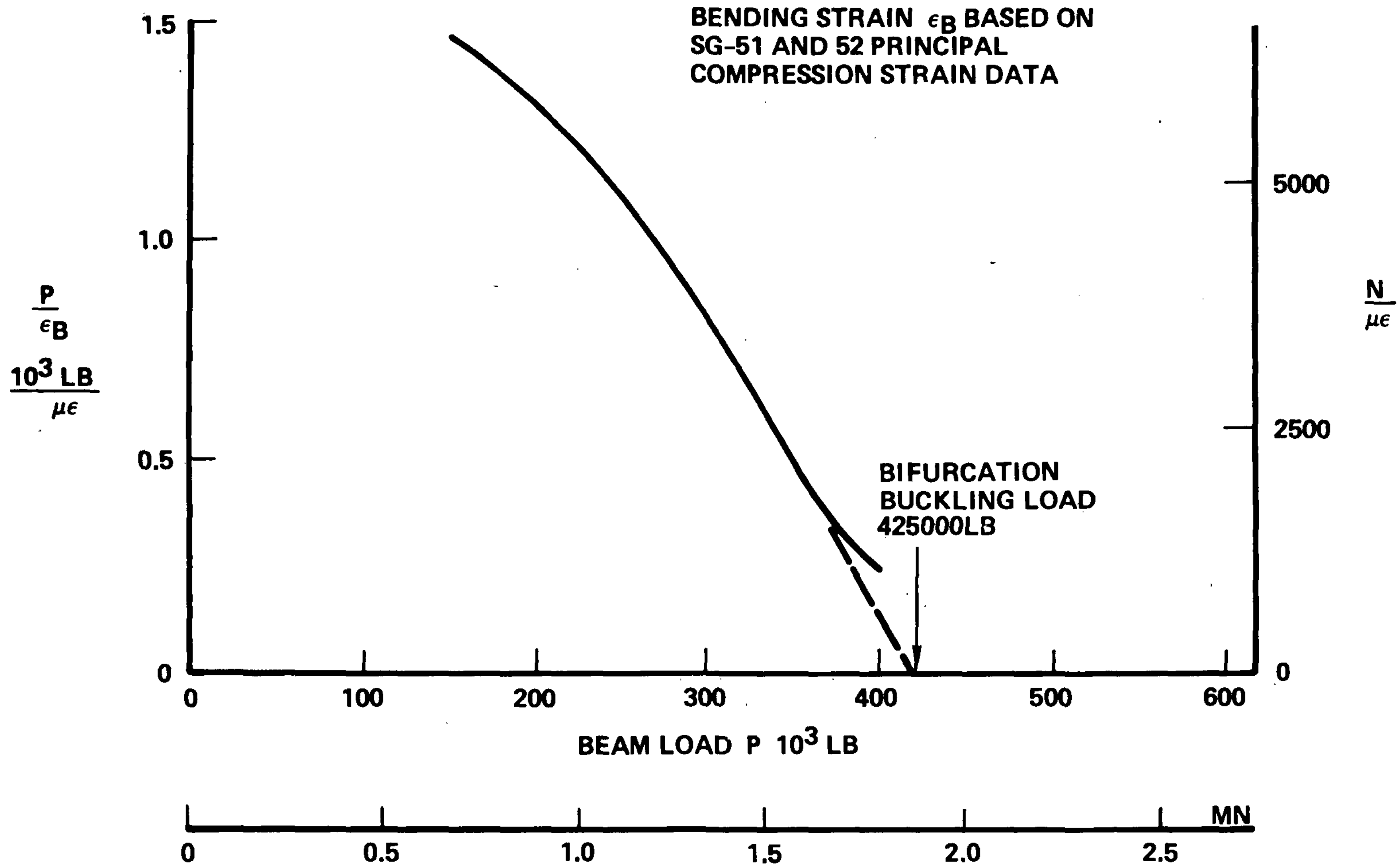

Figure 35: FORCE/STRAIN PLOT FOR TEST WEB 2 INITIAL LOADING

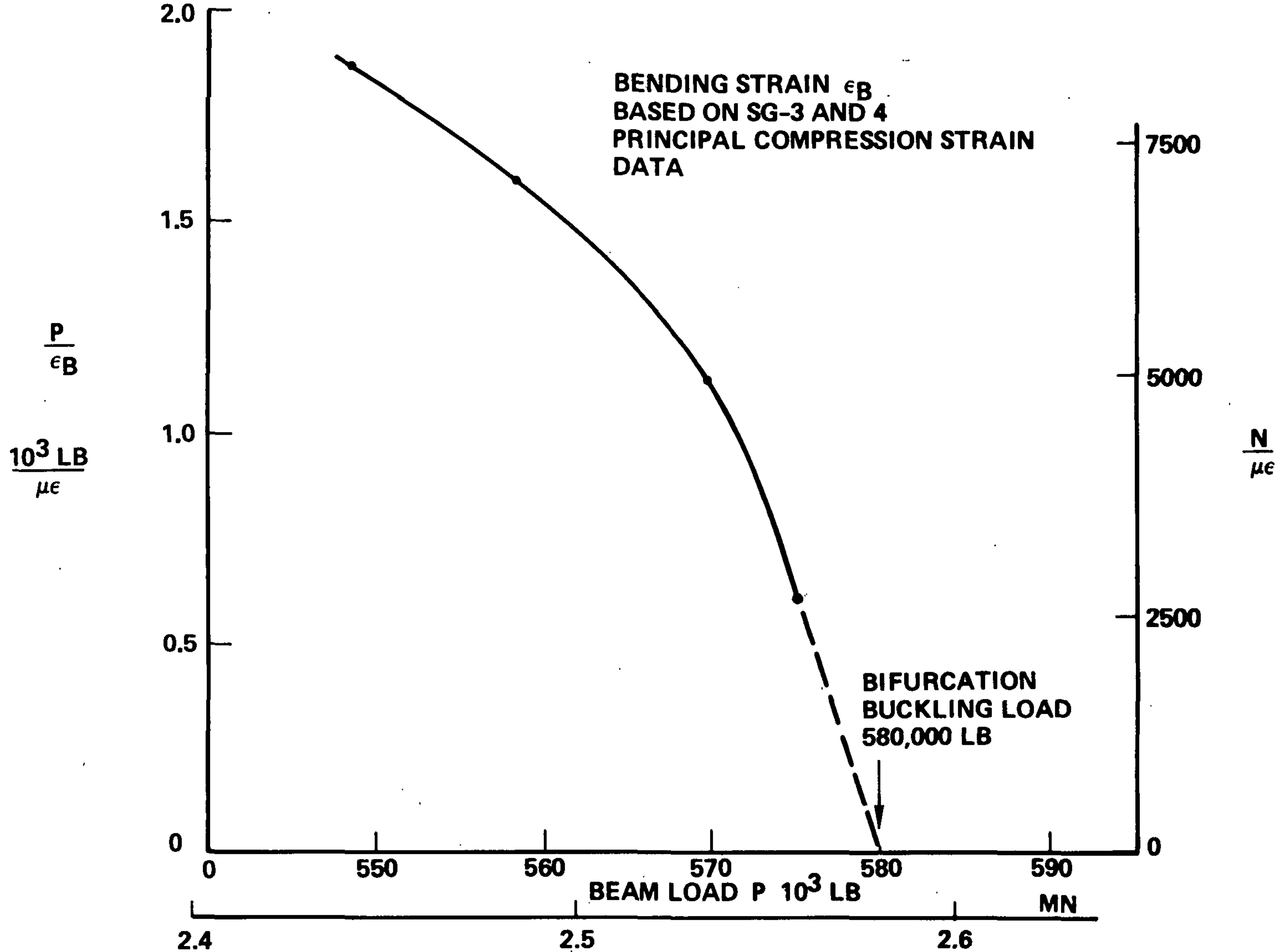

Figure 36: FORCE/STRAIN PLOT FOR TEST WEB 3 FINAL LOADING

possible rather than the final loading. The final loading response is generally different (gives a higher extrapolated buckling load) because of cyclic load effects on initial imperfections and internal load distributions. The development of large deflection and postbuckling response is clearly displayed where the F/S plots diverge from the linear prebuckling condition.

The F/S plot and equivalent definition of bifurcation buckling load can also be obtained directly from Moire fringe data; Figure 37 is a force/moire fringe plot for the third test web. The plot was constructed by counting fringe orders (N_{MF}) from a reference point to the critical buckle peak and then using N_{MF} as an index in place of bending strain in place of the ϵ_B used for the preceding F/S plots.

6.3 LINEAR BUCKLING ANALYSES

The results of the three web tests were correlated with the results from computer-aided buckling analysis of simplified web configurations. In computing structural stiffnesses needed for the buckling analyses, detail dimensions shown in Figures 38 to 40 were used. Dimensions were determined from measurements of the fabricated hardware. The values shown for laminate part thicknesses are average values; small variations occurred due to chem-mill tolerances, resin flow and stock material tolerances. Since the variations were small, the structural analysis results reported herein are based on the dimensions shown.

The computed structural stiffnesses used in the buckling analyses are presented in Figure 41. These stiffnesses were computed by classical laminate analysis and conventional engineering analysis. Bending stiffness tests were conducted on specimens cut from the first and third test webs to verify selected computed values. Also, bending tests were performed on selected stiffeners from the test webs to verify the computed bending stiffnesses. The calculated torsional stiffness for the stiffeners on the first test web was verified by torsion testing. In calculating stiffener stiffnesses, none of the web laminate nor web-to-stiffener eccentricity effects were included.

An existing Ritz energy buckling solution was modified for analysis of the test webs. This solution was developed in support of the Boeing SST Program for use in computing bifurcation loads of simply supported, transversely stiffened, orthotropic shear webs [6]. Coding for this solution was extended to treat beam bending and longitudinal stiffening such as used on the third test web; the modified code is called the WEBBUC code [3].

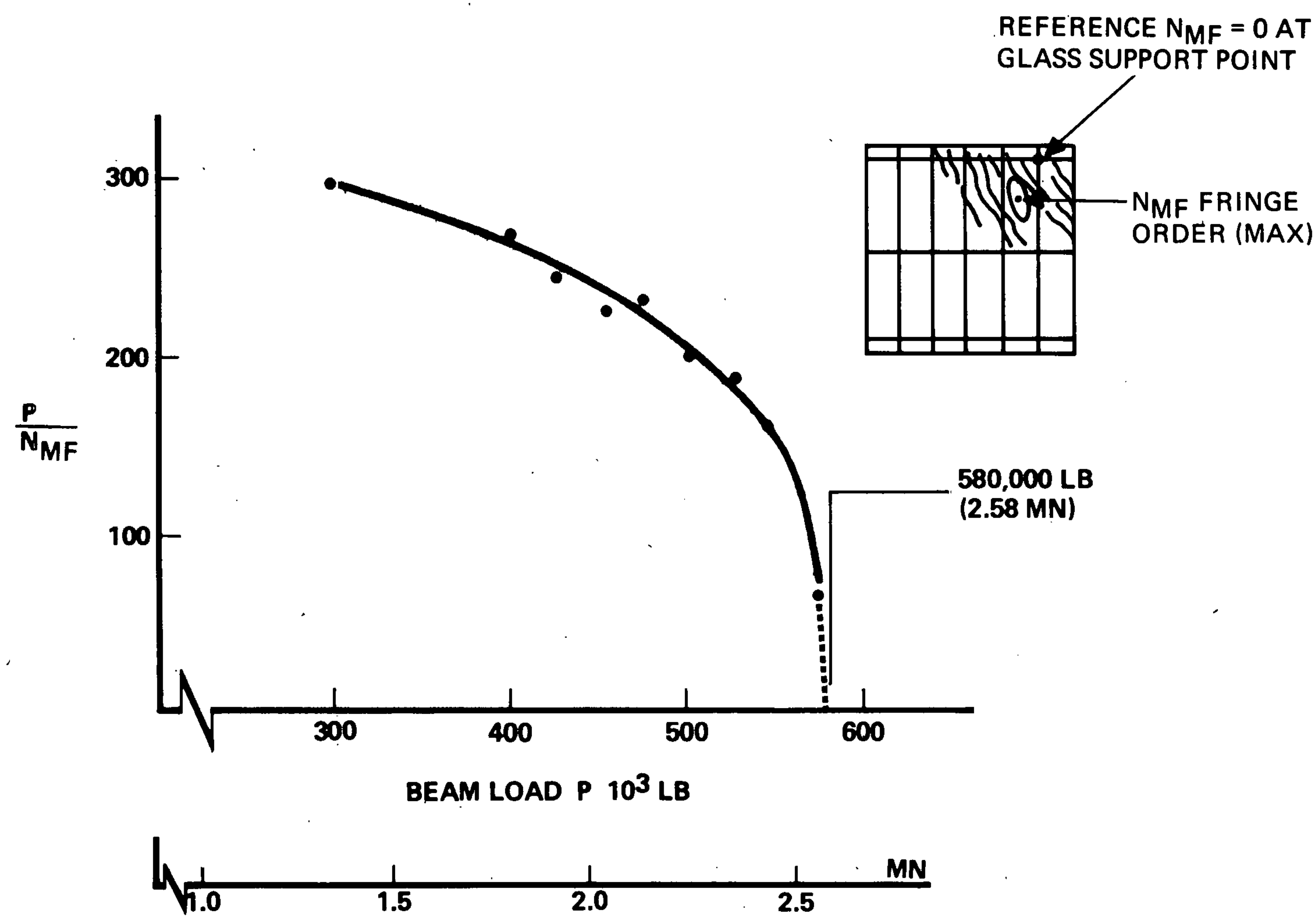

Figure 37: FORCE/MOIRE FRINGE PLOT FOR TEST WEB 3 FINAL LOADING

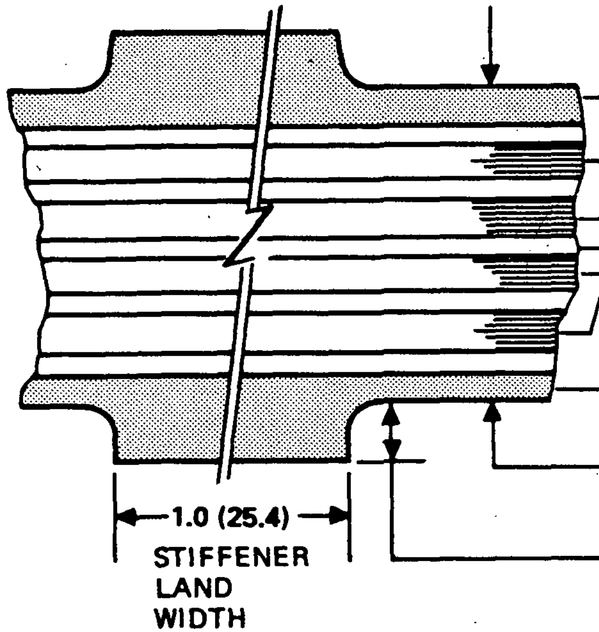

	TEST WEB COMPONENT		
	TW-1	TW-2	TW-3
6AL-4V Ti M.A. CLADDING	0.022 (0.559)	0.022 (0.559)	0.0195 (0.495)
±45° B/E NARMCO 5505/4 16 PLIES @	0.0052 (0.132)	0.0052 (0.132)	0.0051 (0.132)
METLBOND 329 ADHESIVE NO. PLIES	5	6 [1]	5
PLY THK.	0.011 (0.279)	0.011 (0.279)	0.009 (0.229)
6AL - 4V Ti M.A. CLADDING	0.022 (0.559)	0.022 (0.559)	0.0195 (0.559)
NOMINAL LAMINATE THICKNESS	0.1822 (4.628)	0.1932 (4.907)	0.1656 (4.206)
CLADDING REINFORCEMENT PAD-UP AT STIFFENERS	0.030 (0.762)	0.030 (0.762)	0.030 (0.762)
TRANSVERSE STIFFENER SPACING	6.0(15.24)	6.0(15.24)	5.0(12.7)

UNITS
IN (mm)

Figure 38: WEB LAMINATE FABRICATED DIMENSIONS USED IN STRUCTURAL ANALYSES

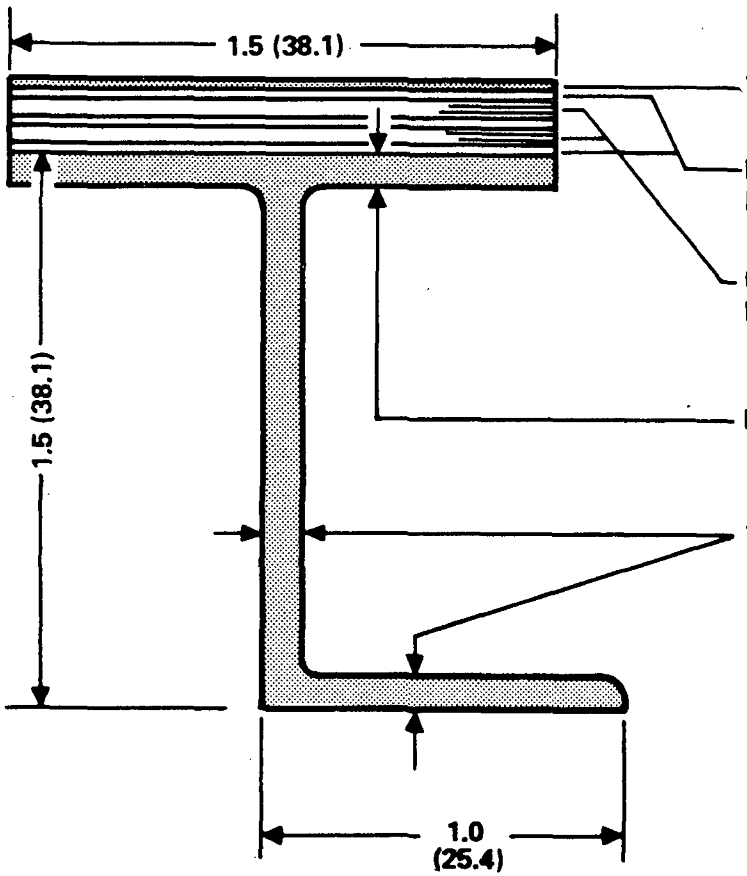

	TEST WEB COMPONENT		
	TW-1	TW-2	TW-3
7075-T6 AL.	0.020 (0.508)	0.020 (0.508)	0.020 (0.508)
BMS 5-51, TYPE 2, GD-5 EPOXY ADHESIVE 2 PLIES @	0.003 (0.0762)	0.003 (0.0762)	0.003 (0.0762)
UNIDIRECTIONAL B/E NARMCO 5505/4 8 PLIES @	0.0052 (0.132)	0.0052 (0.132)	0.0052 (0.132)
FLANGE THICKNESS	0.020 (0.508)	0.125 (3.175)	0.030 (0.762)
7075-T6 AL. STIFFENER	0.09 (2.286)	0.125 (3.175)	0.125 (3.175)
STIFFENER SPACING	6.0 (15.2)	6.0 (15.2)	5.0 (12.7)

UNITS
IN (mm)

Figure 39: TRANSVERSE STIFFENER FABRICATED DIMENSIONS USED IN STRUCTURAL ANALYSES

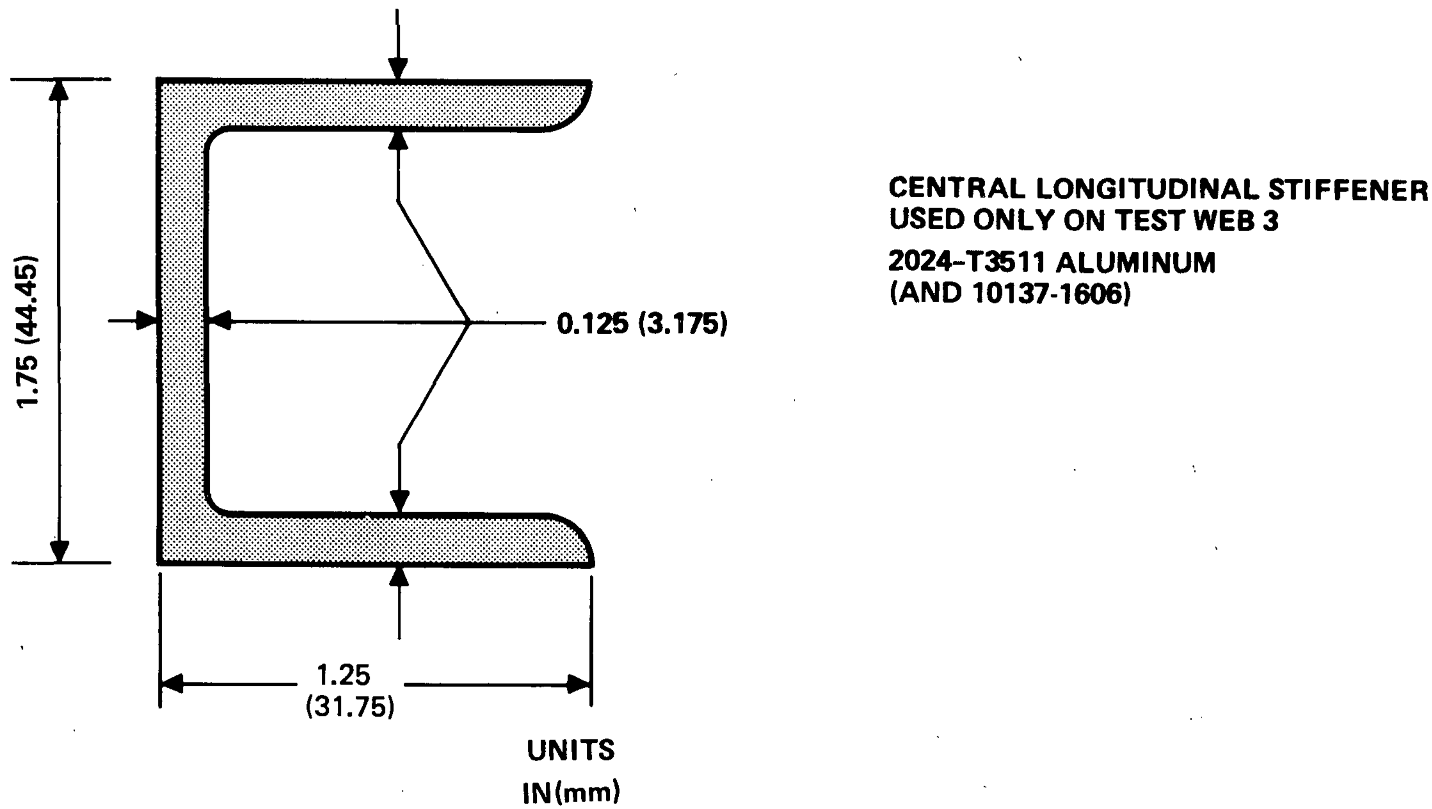

Figure 40: LONGITUDINAL STIFFENER DIMENSIONS USED IN STRUCTURAL ANALYSES

TEST WEB	WEB NOMINAL LAMINATE				TRANSVERSE STIFFENERS		LONGITUDINAL STIFFENER
	D_{11} LB-IN (NM)	D_{12}	D_{22}	[1] D_{33}	EI_T LB-IN^2 (NM^2)	GJ_T	EI_L
1	6023.1 (680.5)	2270.5 (256.5)	6023.1 (680.5)	2610.1 (294.9)	1.483E6 (4256.)	7500 (21.5)	NONE
2	7024.3 (793.6)	2705.9 (305.7)	7024.3 (793.6)	3105.4 (350.9)	1.77E6 (5080.)	20000 (57.4)	NONE
3	4536.4 (512.5)	1749.9 (197.7)	4536.4 (512.5)	2008.9 (227.0)	1.64E6 (4706.)	15000 (43.0)	2.41E6 (100% EFFECTIVE VALUE) (6926.)

[1] D_{33} WOULD BE DEFINED IN ISOTROPIC TERMS AS $\frac{Gt^3}{12}$

Figure 41: STRUCTURAL STIFFNESSES USED IN STRUCTURAL ANALYSES

Numerous analyses were performed using the WEBBUC code in which the height of an effective, simply supported web was varied. Figures 42 to 44 show the computed critical shear buckling loads versus effective web height for the respective test webs. Also shown are the test shear loads given by dividing the bifurcation buckling loads, defined by the F/S data (Section 6.2), by the total web height.

Both test webs 1 and 2 appear to have effective web heights on the order of the nominal laminate panel height. The reason for this is buckling occurs in the central portion of the high aspect ratio panels and is not significantly influenced by the web edge conditions.

Test web 3, having a longitudinal stiffener, had smaller panels and the test data indicates panel deflections occurred near the beam chords, therefore the effective web height lies between the nominal laminate height and the clear height between chord angles. Because of the large cut-outs that were present in the longitudinal stiffener, the stiffness of this stiffener was not fully effective. Assuming a 50% longitudinal stiffener effectiveness results in an effective web height of 29 inches when comparing the test versus the predicted buckling loads in Figure 44. This correlation is, of course, subject to interpretation. In a future analysis situation, one would be conservative to compute the buckling load based on the full clear web height and some reduced effective longitudinal stiffener stiffness.

In all of the correlation studies, it was found that satisfactory correlation could only be obtained when stiffener stiffnesses were calculated on the basis of an uncoupled stiffener section, neglecting the web laminate parts and web-to-stiffener eccentricity. An explanation of this is that the stiffener/web assembly fasteners were non-hole filling and were not tightly torqued (to preclude damaging the web laminate) which does not provide a strong shear-tie. During buckling deformation, slippage probably occurred between the stiffeners and the web so that the stiffeners were loaded primarily in bending. In a production program, studies of fastening methods should be undertaken to improve stiffener/web interaction.

Beam bending loads were included in the buckling analysis of the third test web, as shown in Figure 44. In a separate shear/bending interaction study, the effects of the test beam bending on the critical shear buckling load was found to be insignificant because of the low magnitude of chord strain due to beam bending. While the test webs had low beam bending loads, the effects of load interaction must not be neglected in buckling analysis of "shear resistant" production webs which can have high beam chord strains.

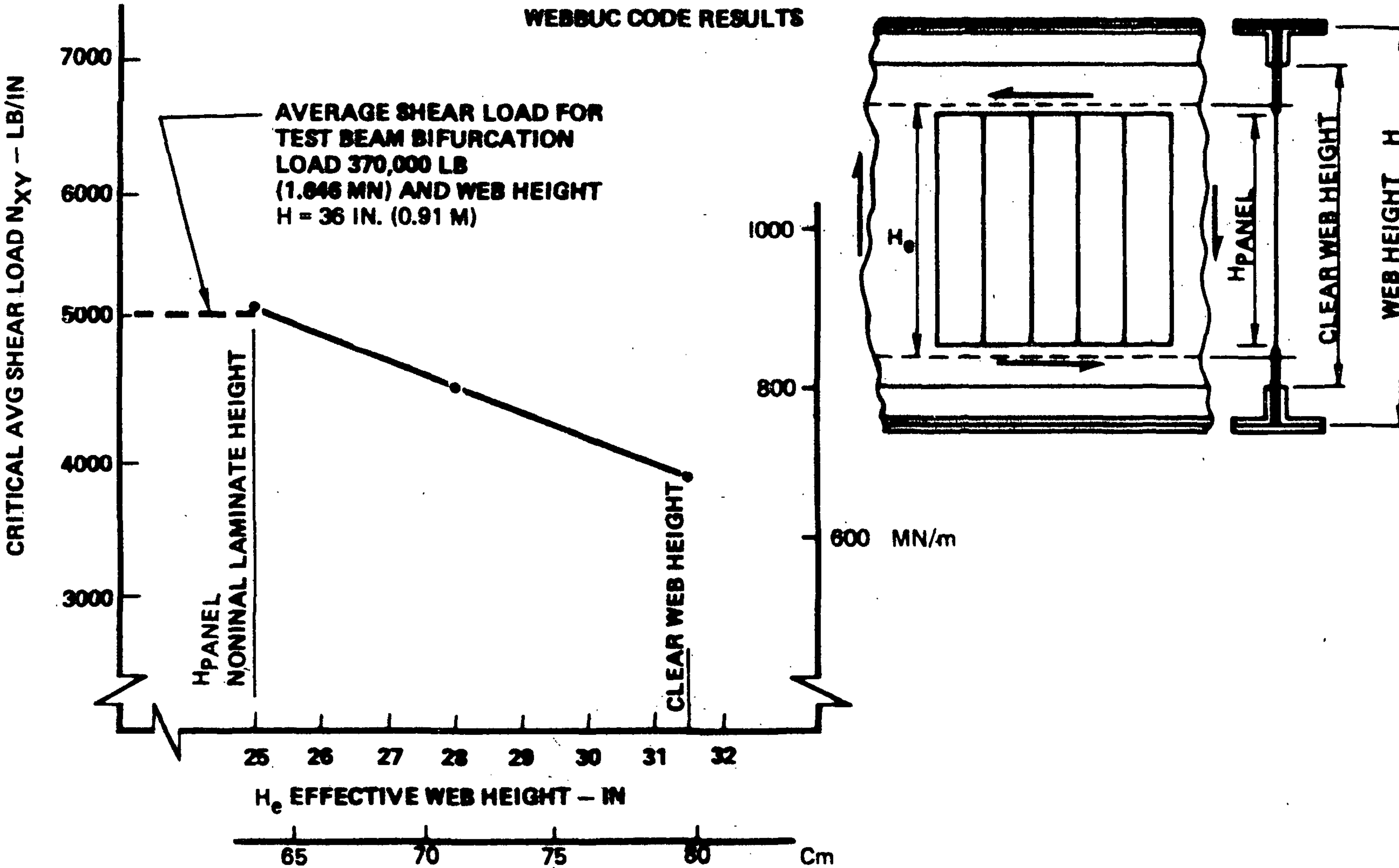

Figure 42: BUCKLING ANALYSIS/TEST CORRELATION FOR TEST WEB 1

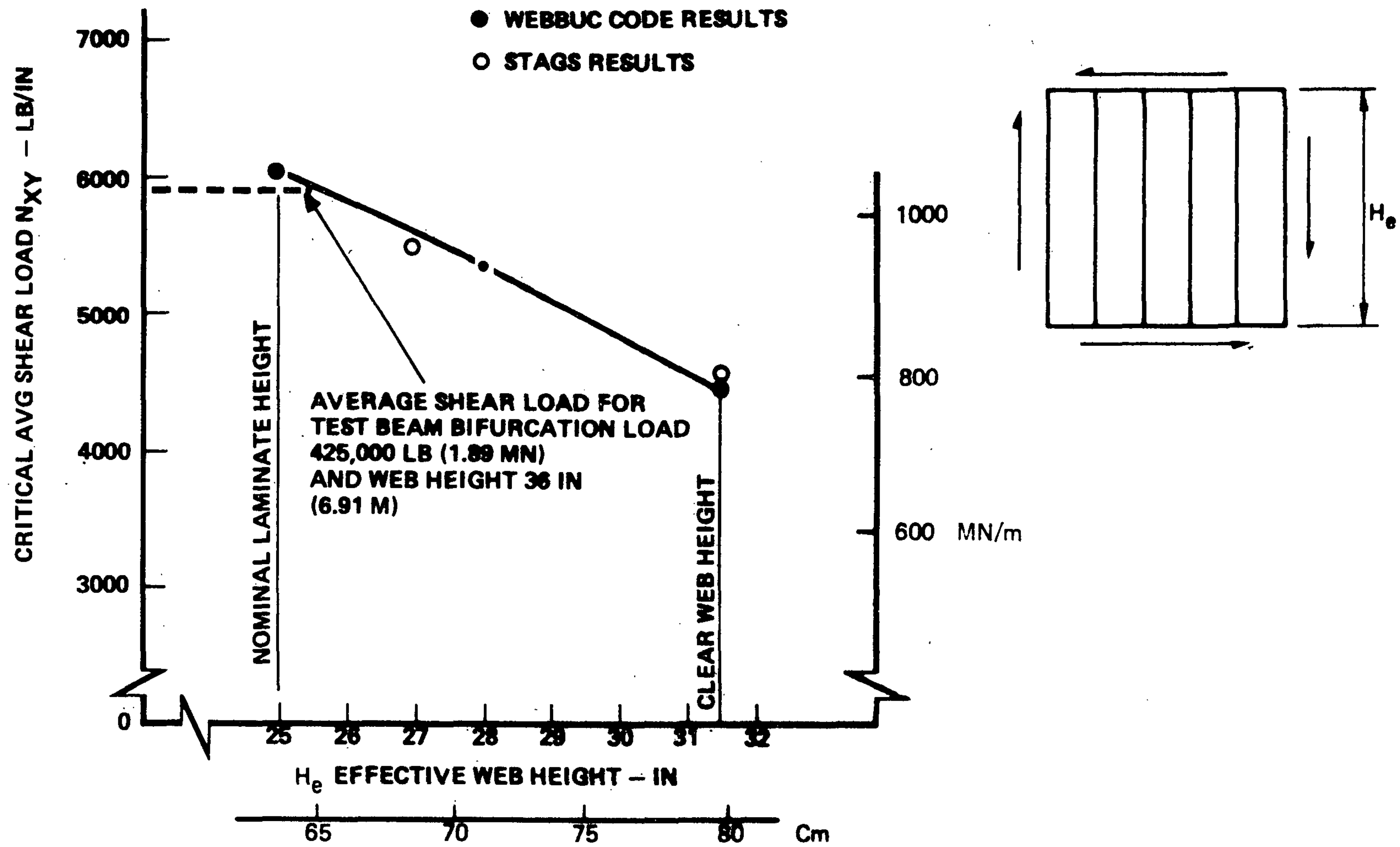

Figure 43: BUCKLING ANALYSIS/TEST CORRELATION FOR TEST WEB 2

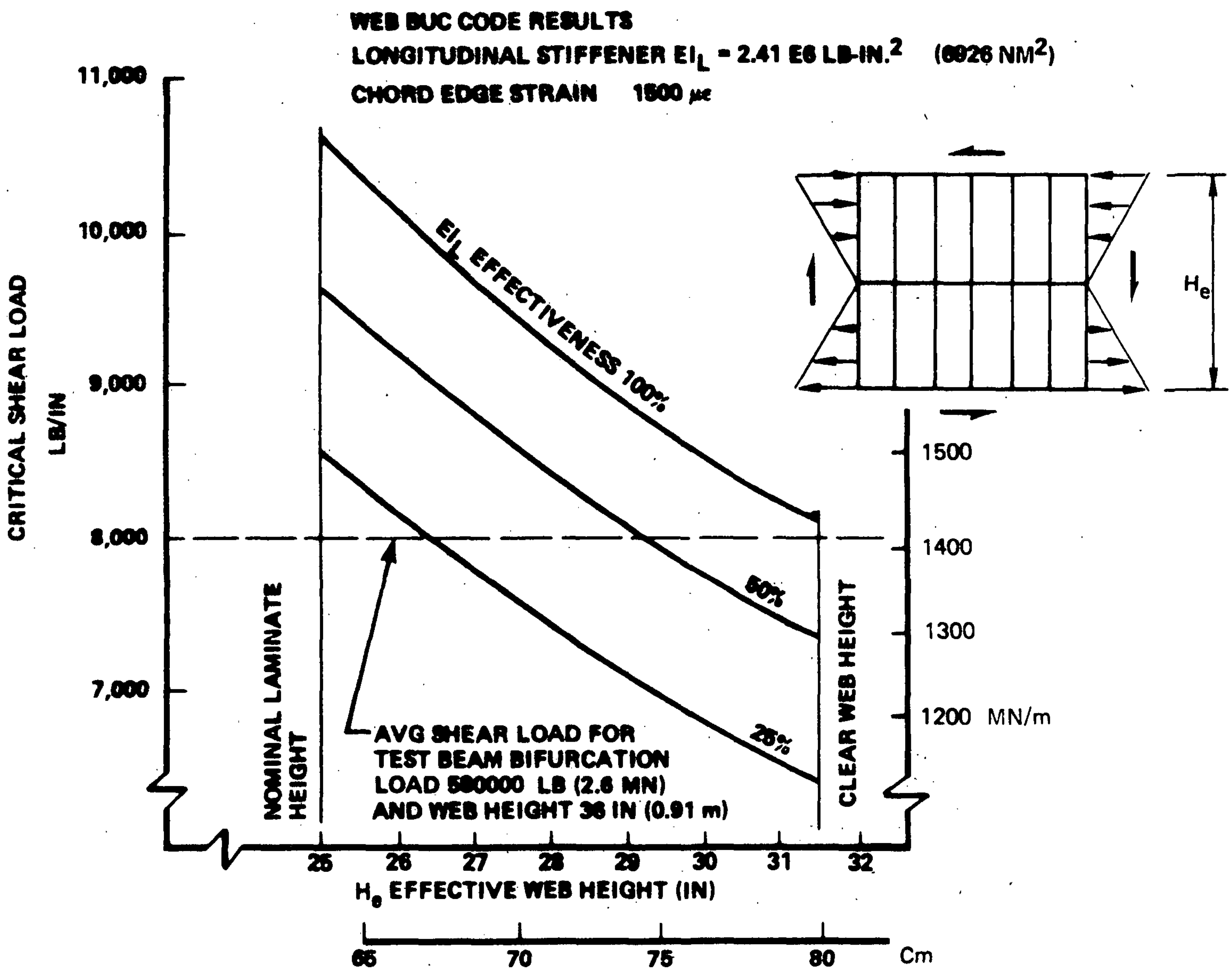

Figure 44: BUCKLING ANALYSIS/TEST CORRELATION FOR TEST WEB 3

In Figure 43, some linear buckling analysis results from the STAGS code [7] are shown. The STAGS code is based on a finite difference energy solution approach; its use in analysis of production hardware is recommended. A particularly useful feature of the STAGS code is its capability to perform non-linear pre and postbuckling analyses in an efficient manner. For the STAGS analyses shown, the input structural properties (orthotropic laminate stiffnesses, etc.) were the same as used in the WEBBUC code analyses and web configurations having four panels were treated.

6.4 BUCKLED PANEL STRAIN DATA ANALYSES

The Moire fringe data was used to compute peak strains in the critical buckled panel areas. The computed strains were compared to measured principal strains and a correlation was found for the prebuckling strains of the test webs. In the case of the third web, the strain data computed from Moire fringe data was useful in establishing failure strain conditions in the critical panel where strain gages were not located.

The Moire fringe patterns from the web tests were analyzed by a curve fitting procedure to establish the strain conditions precisely at the critical buckle peaks. This strain data was characteristically similar to the strain data obtained from the strain gages in close proximity to the critical buckles and was used in subsequent analysis activities.

Figure 45 shows the critical buckle area in the third web at the failure load. The deflected surface was surveyed in the principal compression strain direction to establish coordinates of the fringe orders; both manual surveying and electronic data digitizing equipment (Bendix Digitizer) were employed in the surveys. The coordinate and fringe order calibration data were fitted to a deflection function of the form shown in the figure; the fitting was done by manual and computer aided methods. A wavelength of $\sqrt{2}$ times the stiffener spacing was an assumed deflection function parameter. By differentiating the deflection function twice, the panel bending curvatures were established; local strains at a laminate material point were computed as the product of bending curvature and the coordinate of the material from the neutral laminate surface.

Figures 46 to 48 show strains computed for the test webs. As shown in the figures, the total strain at a given point in the laminate is the superposition of membrane strain and bending strain computed from Moire fringe data. Good qualitative agreement was obtained between the computed strain response and the strain gage data in the prebuckling strain region. In

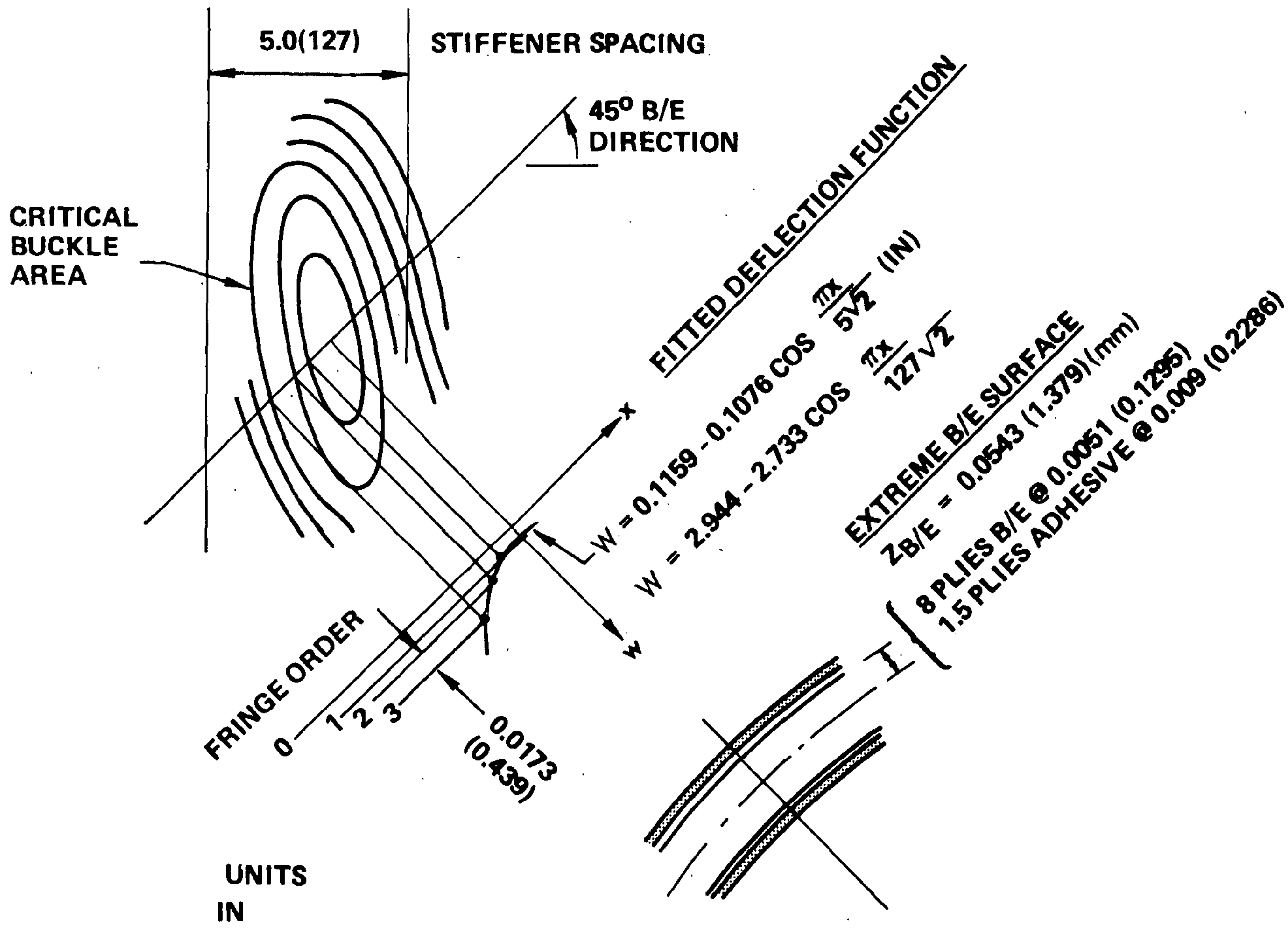

Figure 45: DEFLECTION FUNCTION FITTED TO TEST WEB 3 MOIRE FRINGE DATA

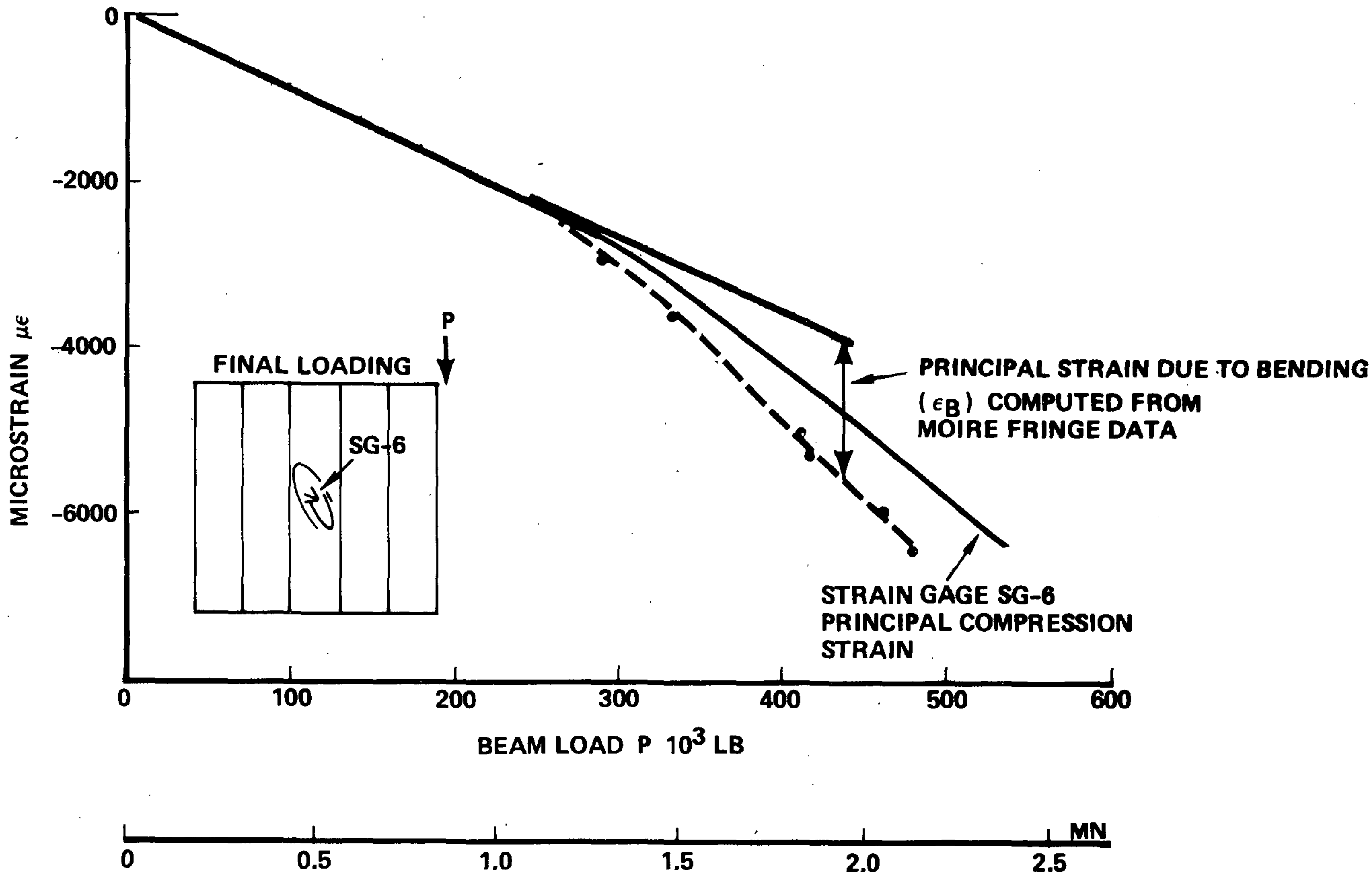

Figure 46: SURFACE CLADDING STRAINS IN TEST WEB 1 CRITICAL BUCKLE AREA

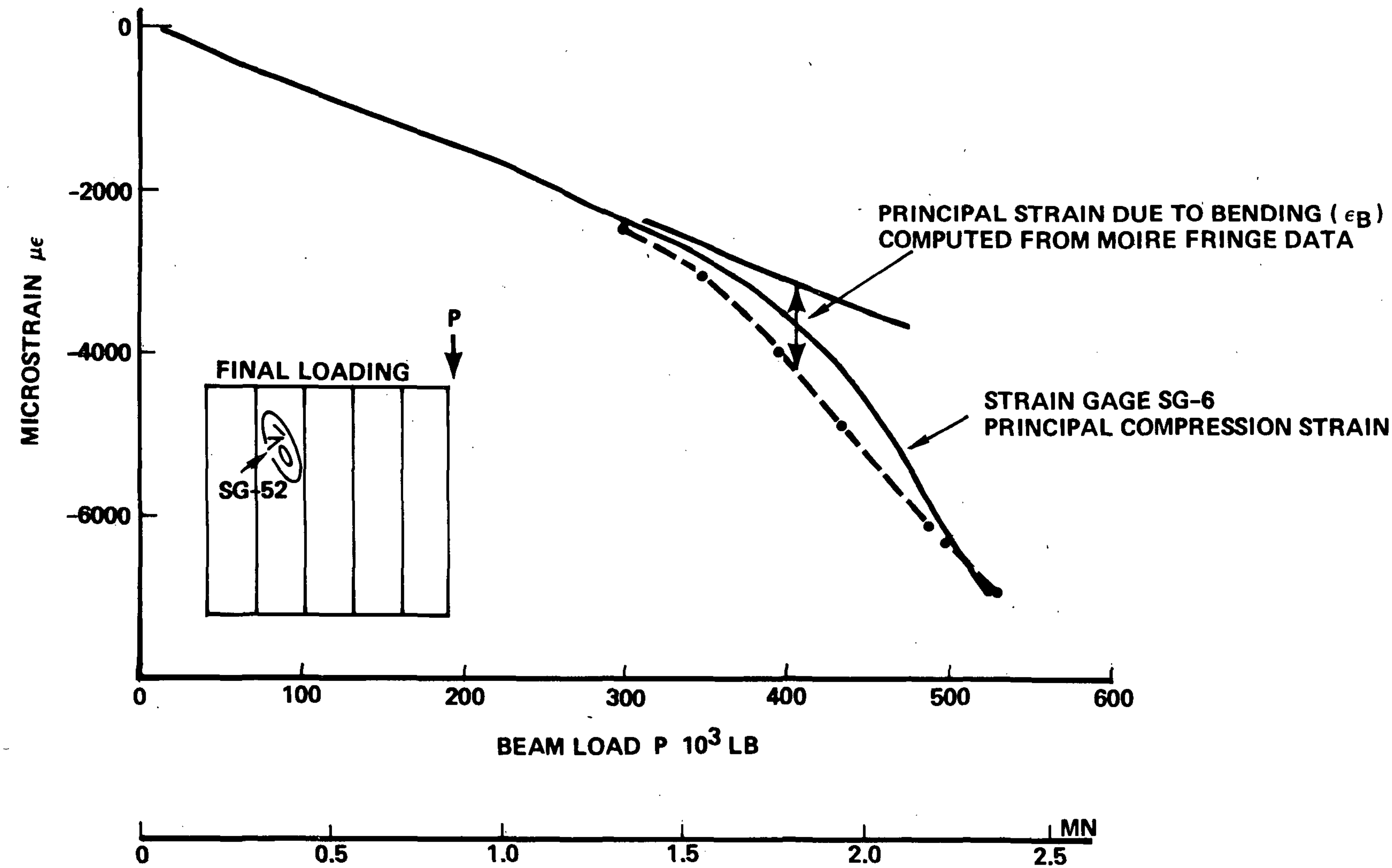

Figure 47: SURFACE CLADDING STRAINS IN TEST WEB 2 CRITICAL BUCKLE AREA

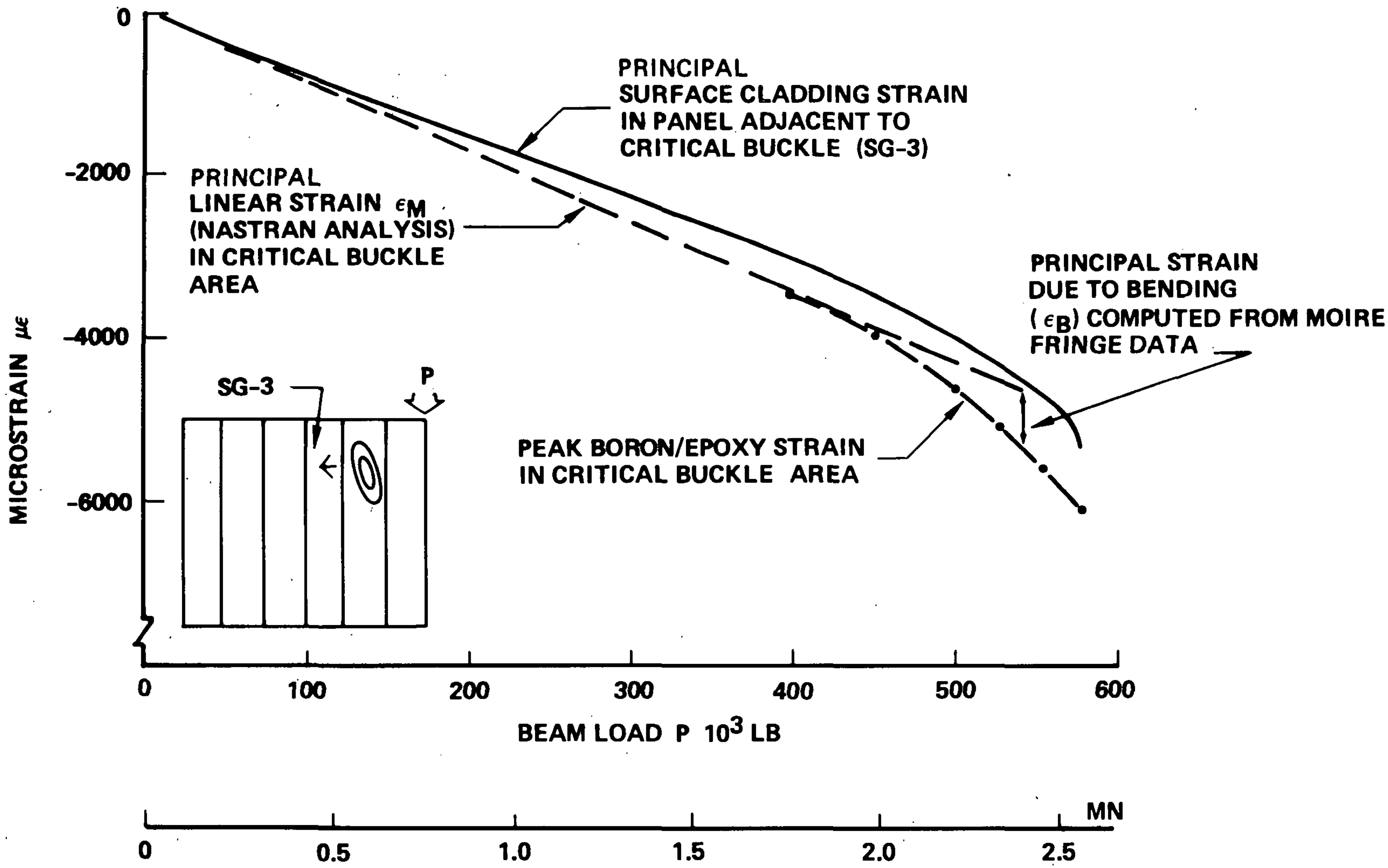

Figure 48: STRAINS IN TEST WEB 3 CRITICAL BUCKLE AREA

general, the computed strains are higher than the measured data. The reason for this is considered to be due to the strain gages not being applied exactly at the peaks of the panel buckles. In tests one and two, the membrane strain response was taken as the initial linear strain gage data. For test web 3 [3], the membrane strain response was computed from data generated using the NASTRAN code; this was done to account for increased internal loads near the loading area where strain gages were not applied. The NASTRAN code, level 15 [8], Boeing Computing Services version with SAIL input preprocessor was used for this purpose.

Test webs 1 and 3 failed by B/E fracture in their respective peak buckling areas. This conclusion is based, in the case of the first web, on the strain response shown in Figure 46 and the data from the companion back-to-back strain gage (Figure 21). These data were used to compute the strains at the extreme B/E plies in the web laminate. The peak B/E strains were in excess of $6000\mu\epsilon$, the typical design allowable strain for the particular B/E material used in the web.

An estimate of the "membrane" strength of the third test web can be made from Figure 48 by projecting the linear strain response plot from the NASTRAN analysis to the $6000\mu\epsilon$ level; this gives a failure load of about 680,000 lb (3.02 MN) based on the assumed critical strain of $6000\mu\epsilon$ for the B/E material. The membrane strength, or the strength of a fully stabilized web laminate, gives an indication of the effectiveness of the web stiffening system. In the case of the third web, the actual failure load was 16% less than the estimated membrane strength which is indicative of a high degree of stiffening performance. Any improvements in stiffener/web interaction in a production web, as discussed in Section 6.3, would serve to improve stiffening performance and allow a reduction in stiffener weight.

Test web 2, during the 400 cycle loading to the "limit" load level, displayed panel surface strains shown in Figure 47 slightly in excess of $4000\mu\epsilon$ in the peak pre-buckled panel areas. This level of cyclic loading produced no apparent damage in the second test web.

7.0 STRUCTURAL ANALYSIS OF TEST WEB 3

Results from a structural analysis of test web 3 are presented in this section. The analysis model and methods used, while preliminary in nature, serve to identify the various analysis considerations that pertain to the metal-clad composite shear web design concept.

The shear buckling resistant qualities that are desired for shear web efficiency, introduce complexities in the analysis to the extent that the analysis is very configuration dependent. Therefore, the structural analysis presented here is intended to show failure mode sensitivity and structural parameters only for the third test web. Structural analysis of other configurations of the design concept will require different or modified analytical techniques, although the primary objective should not change–analysis of strains in prebuckled panels to establish composite fracture and/or metal yielding failure mode margins of safety.

7.1 STRUCTURAL ANALYSIS MODEL

The structural model used for analysis simulated test web 3 with respect to details for the nominal web laminate section, laminate cladding reinforcement for stiffener fasteners, and transverse and longitudinal stiffeners; the structural analysis details and equations are given in Reference [3]. The analysis model was coded as a special version of the Boeing OPTRAN code [3] which was operated in an "analysis only" mode to analyze the third test web. The analysis was conducted with a prescribed set of structural dimensions for test web 3 given in Figures 38 to 40. Because of the highly skewed form of the panel buckling mode (refer to the Moire fringe pattern in Figure 31), a "long" web simulation of the test web could be adopted.

Figure 49 shows the "shear resistant" web loads (shear load and beam chord strain) that were input data to the OPTRAN code. The bending strain loads at the beam chords are corrected linearly to levels at the assumed edge of the nominal laminate panel and at interior panel points for use in structural analyses. The loads used in the structural analysis were the test loads at failure: a shear load of 287,500 lb (1.28 MN) and an average chord strain of $1500\mu\epsilon$ which was established by finite element analysis.

The pre-buckled panel strains were analyzed at a location shown in Figure 50; this location was selected based on recognition of beam bending loads and their possible influence on shifting the panel buckle towards the compression chord (as occurred in the third web test,

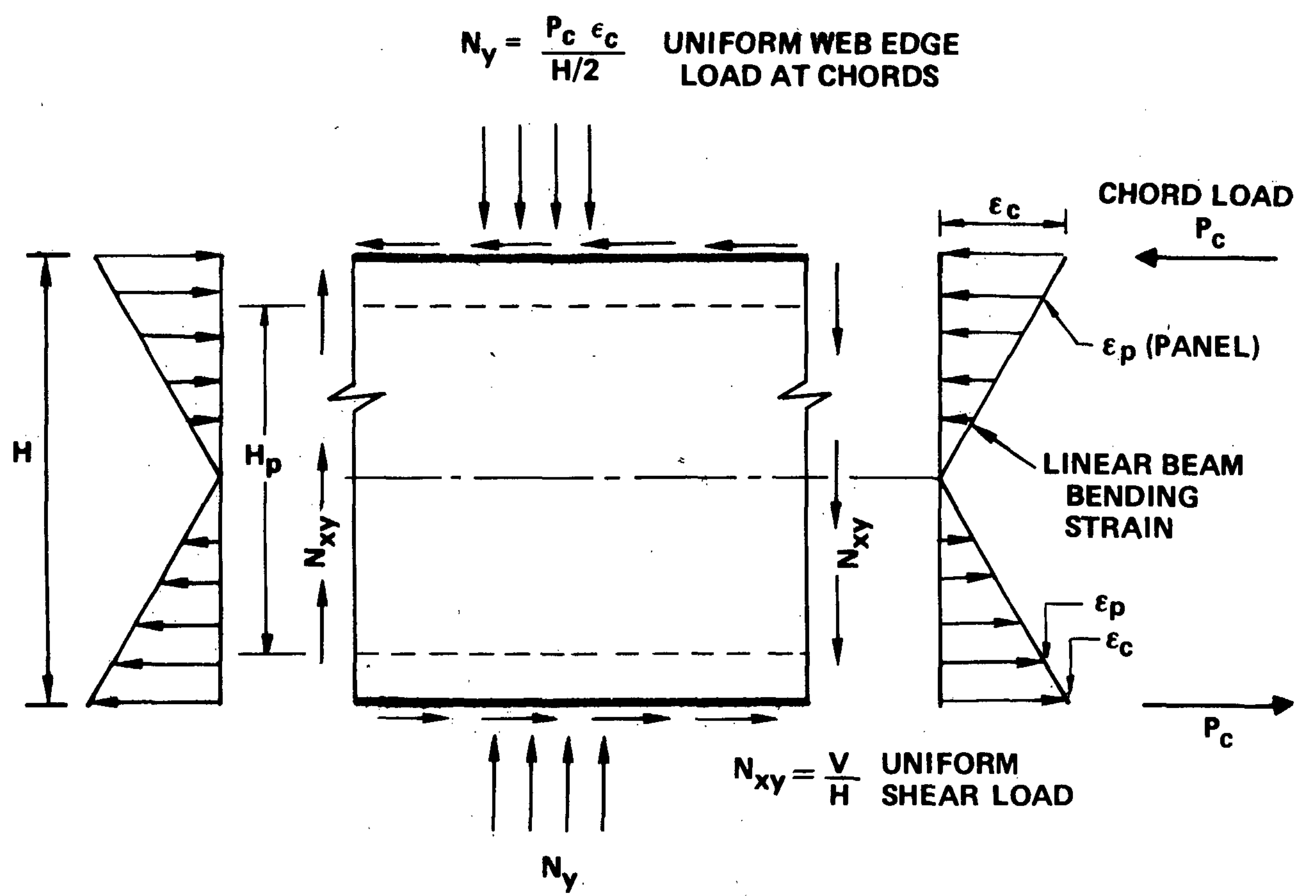

Figure 49: SHEAR RESISTANT WEB LOADS

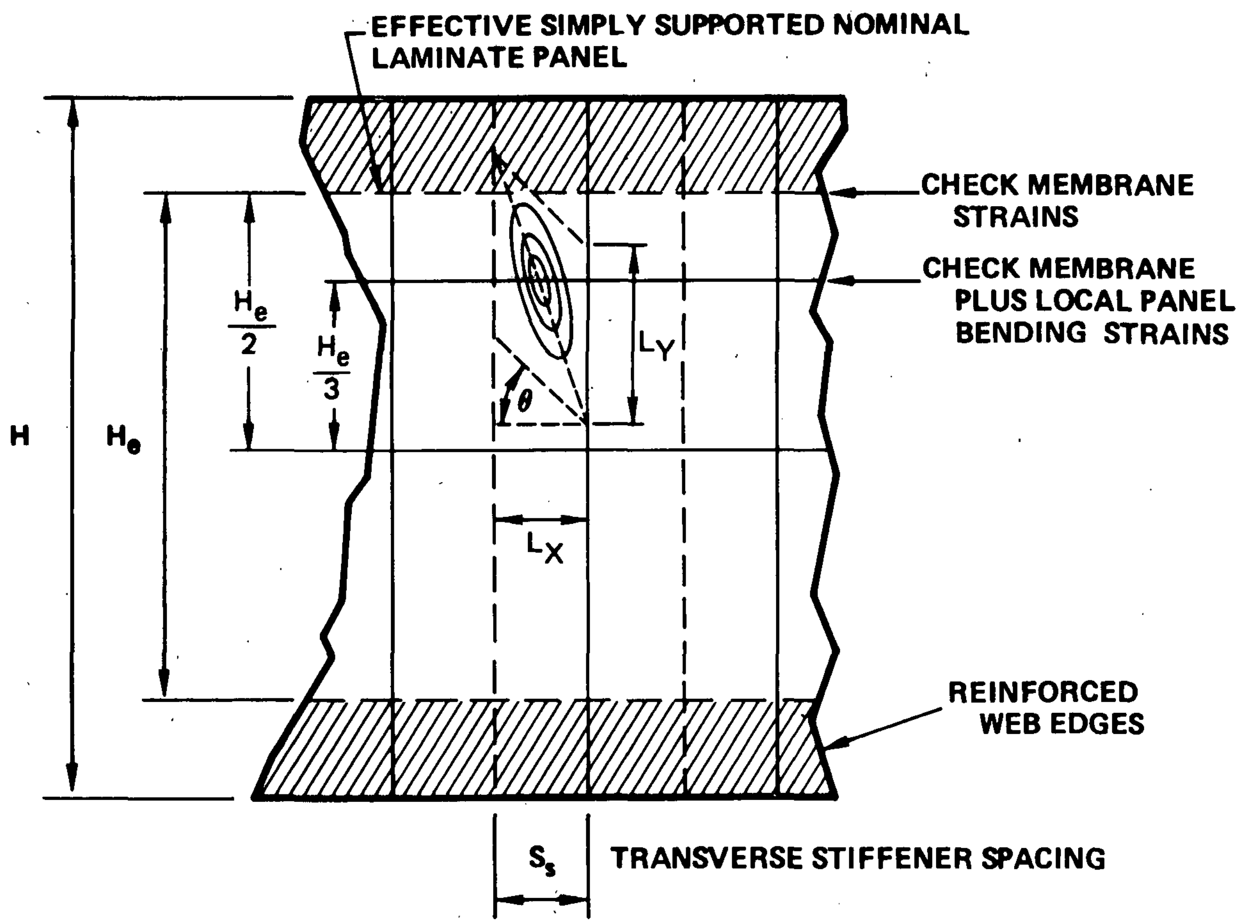

Figure 50: LAMINATE STRAIN ANALYSIS LOCATIONS

see Figure 31). In addition to the buckle peak area, strain analysis was conducted at the assumed effective nominal laminate panel edge where the membrane strains are maximum. Out-of-plane web plate bending strains were assumed to be zero at the effective nominal laminate panel edge. The assumed prebuckled panel deflection mode parameters for wave lengths (L_X and L_Y) and skew angle (Θ) shown in Figure 50 were estimated from the Moire fringe pattern at the failure load [3]; the estimated values used were L_X = 5.0 inches (12.7 cm), L_Y = 14.0 inches (35.6 cm) and $\Theta = 60^o$. The prebuckled panel initial deflection was defined by an assumed initial imperfection magnitude of 0.003 inch (0.076 mm). This magnitude is within the fringe order sensitivity for the Moire fringe pattern in the critical panel area at zero load shown in Figure 27. After web assembly, surveys made with a feeler gage and a straight edge in the critical area indicated that the deviation from flatness was on the order of the assumed imperfection level.

An effective panel height of 25 inches (63.5 cm) was assumed for the structural analysis. This height, which was the actual nominal web laminate panel height, is less than the effective panel height defined by the linear buckling analysis described in Section 6.3. The assumed panel height value was necessary to produce a positive margin of safety for web buckling using the analyses given in the Appendix of Reference [3]; these buckling analyses are conservative in the case of the third test web.

7.2 STRUCTURAL ANALYSIS RESULTS

The margins of safety computed for the various possible failure modes of test web 3 are as follows:

Buckled nominal laminate panel area:	
Cladding yielding	+0.09
Composite strain	+0.01
Unbuckled nominal laminate panel edge area:	
Cladding yielding	+0.19
Composite strain	+0.18
General web instability	+0.11
Web tearing at stiffener fastener holes	+0.15

The critical computed margin of safety is for composite strain in the pre-buckled panel area; a higher positive margin of safety exists with respect to failure by titanium cladding yielding. These results are in agreement with the test strain data analysis in Section 5.2

which indicates that failure of test web 3 occurred by fracturing of the B/E in a pre-buckled panel. The structural analysis assumed a critical B/E strain of 6000$\mu\epsilon$ and the test data analysis shows the actual strain at failure was slightly in excess of that value. The computed margin of safety for general web instability is positive and is in agreement with the pre-buckling conditions developed in the test.

Adequate margin of safety was computed for the web laminate in the edge area and along the reinforced stiffener fastener holes.

8.0 EVALUATION CONCLUSIONS

The titanium-clad B/E reinforced shear web design concept is considered to be practical and efficient for the specific application that was evaluated. The test web components used for evaluation generally performed satisfactorily under low-cycle loadings.

The first and third test webs failed in mid-panel areas due to panel buckling conditions; in future production hardware, the failure conditions can be predicted with the aid of existing analysis tools [3] but not without difficulty. The results from the first test indicate the concept has a lack of postbuckling strength since postbuckling strains are limited by the brittle nature of the composite laminate material. The benefits of a shear buckling resistant design approach to web efficiency is evident from the results of the third test. The third web failed at a load just below the classical linear buckling load; the failure load was only about 16% less than the theoretical load capability of a fully stabilized web laminate. Confident load capability prediction and laminate/stiffening optimization for shear resistant design in future hardware will require that special analytical and element test techniques be developed and employed. Specifically, convenient prebuckling analysis methods and design aids must be developed before the concept can be easily applied in structural designs.

The structural details of the second test web were apparently unaffected by application of just over 400 "limit" load cycles. Based on this low-cycle fatigue test (a "worst" case test due to a high level of prebuckling panel deformation that occurred during cyclic loading) and structural element fatigue tests [1], the high-cycle fatigue resistance of the concept will probably be determined by the fatigue properties of the web laminate's metal cladding.

The metal-clad web laminate is an attractive concept because of the protection offered by the cladding to the polymeric laminate parts and the low-cost tooling and inspection operations needed in its fabrication. The metal cladding, because of its exterior location, provides effective material in the prevention of panel buckling. This is reflected by the low B/E content in the test web assemblies; the third test web had only 14% of its total web assembly weight as B/E material. In other words, the titanium-clad B/E material concept offers good weight savings, (31% theoretical nominal section weight savings compared to all-metal construction [3]) with only a small amount of B/E composite material required.

An area that requires further investigation in a production program is the method of stiffener attachment. Non-interference fit steel bolts were employed in the test web assemblies and these fasteners were not tightly torqued to preclude damaging the web laminate. The test data analysis indicates the stiffeners were not fully shear-coupled to the web laminate. The use of interference fit fasteners will make the stiffeners fully effective in both bending and extension which will result in increased stiffener efficiency (increased shear buckling resistance). Further studies may also identify stiffener configurations more optimum than used on the third test web as a consequence of the production stiffener attachment method [3].

9.0 REFERENCES

1. NASA CR-132320, "Evaluation of a Metal Shear Web Selectively Reinforced With Filamentary Composites for Space Shuttle Application–Phase I Report", J. H. Laakso and D. K. Zimmerman, Prepared under NASA/LRC Contract NAS1-10860, Boeing Aerospace Company Document D180-15104, September 1972.
2. NASA CR-132321, "Evaluation of a Metal Shear Web Selectively Reinforced With Filamentary Composite for Space Shuttle Application–Phase II Report," J. H. Laakso and D. K. Zimmerman, Prepared under NASA/LRC Contract NAS1-10860, Boeing Aerospace Company Document D180-15323, February 1973.
3. NASA CR-132322, "Evaluation of a Metal Shear Web Selectively Reinforced With Filamentary Composite for Space Shuttle Application–Phase III Report," J. H. Laakso and J. W. Straayer, Prepared under NASA/LRC Contract NAS1-10860, Boeing Aerospace Company Document D180-17566-1, August 1973.
4. B. C. Dykes, "Analysis of Displacements in Large Plates by the Grid-Shadow Moire Technique," Paper 14, Proceedings of the Fourth International Conference on Experimental Stress Analysis, Cambridge, England, 1970.
5. M. D. Musgrove and B. E. Greene, "Advanced Beaded and Tubular Structural Panels," Paper 73-370, AIAA/ASME/SAE 14th Structures, Structural Dynamics, and Materials Conference, Williamsburg, Virginia, March 20-22, 1973.
6. R. M. Mello, M. D. Musgrove and R. E. Sherrer, "Intermediate Diagonal Tension Field Shear Beam Development For the Boeing SST," Paper 71-340, AIAA/ASME/SAE 12th Structures, Structural Dynamics, and Materials Conference, Anaheim, California, April 19-21, 1971.
7. B. O. Almroth, et al, "User's Manual for the STAGS Computer Code," Lockheed Missiles and Space Compant Report LMSC D266611 (STAGS A), October 1972.
8. NASA SP-222, "NASTRAN User's Manual," September 1970.

"The aeronautical and space activities of the United States shall be conducted so as to contribute . . . to the expansion of human knowledge of phenomena in the atmosphere and space. The Administration shall provide for the widest practicable and appropriate dissemination of information concerning its activities and the results thereof."

—NATIONAL AERONAUTICS AND SPACE ACT OF 1958

NASA SCIENTIFIC AND TECHNICAL PUBLICATIONS

TECHNICAL REPORTS: Scientific and technical information considered important, complete, and a lasting contribution to existing knowledge.

TECHNICAL NOTES: Information less broad in scope but nevertheless of importance as a contribution to existing knowledge.

TECHNICAL MEMORANDUMS: Information receiving limited distribution because of preliminary data, security classification, or other reasons. Also includes conference proceedings with either limited or unlimited distribution.

CONTRACTOR REPORTS: Scientific and technical information generated under a NASA contract or grant and considered an important contribution to existing knowledge.

TECHNICAL TRANSLATIONS: Information published in a foreign language considered to merit NASA distribution in English.

SPECIAL PUBLICATIONS: Information derived from or of value to NASA activities. Publications include final reports of major projects, monographs, data compilations, handbooks, sourcebooks, and special bibliographies.

TECHNOLOGY UTILIZATION PUBLICATIONS: Information on technology used by NASA that may be of particular interest in commercial and other non-aerospace applications. Publications include Tech Briefs, Technology Utilization Reports and Technology Surveys.

Details on the availability of these publications may be obtained from:

SCIENTIFIC AND TECHNICAL INFORMATION OFFICE

NATIONAL AERONAUTICS AND SPACE ADMINISTRATION

Washington, D.C. 20546